LLNL-CONF-836814

3D SIMULATIONS CAPTURE THE PERSISTENT LOW MODE ASYMMETRIES EVIDENT IN LASER-DIRECT- DRIVE IMPLOSIONS ON OMEGA

A. COLAITIS, I. IGUMENSCHEV, D. TURNBULL, R. SHAH, D. EDGELL, O. MANNION, D. STROZZI, T. CHAPMAN, C. STOECKL, D. JACOB-PERKINS, A. SHVYDKY, R. JANEZIC, A. KALB, D. CAO, C. J. FORREST, J. KWIATKOWSKI, S. REGAN, W. THEOBALD, V. GONCHAROV, D. FROULA

June 29, 2022

European Physical Society Div. Plasma Physics
virtual, Czech Republic
June 27, 2022 through July 1, 2022

3D SIMULATIONS CAPTURE THE PERSISTENT LOW MODE ASYMMETRIES EVIDENT IN LASER-DIRECT-DRIVE IMPLOSIONS ON OMEGA

EPS-DPP 2022

JUNE 6TH, 2022

A. COLAITIS(1), I. IGUMENSCHEV(2), D. TURNBULL(2), R. SHAH(2), D. EDGELL(2), O. MANNION(3), D. STROZZI(4), T. CHAPMAN(4), C. STOECKL(2), D. JACOB-PERKINS(2), A. SHVYDKY(2), R. JANEZIC(2), A. KALB(2), D. CAO(2), C. J. FORREST(2), J. KWIATKOWSKI(2), S. REGAN(2), W. THEOBALD(2), V. GONCHAROV(2), D. FROULA(2)

1. CELIA, BORDEAUX
2. LLE, ROCHESTER NY
3. SANDIA NATIONAL LABORATORIES*, NM
4. LLNL, LIVERMORE CA

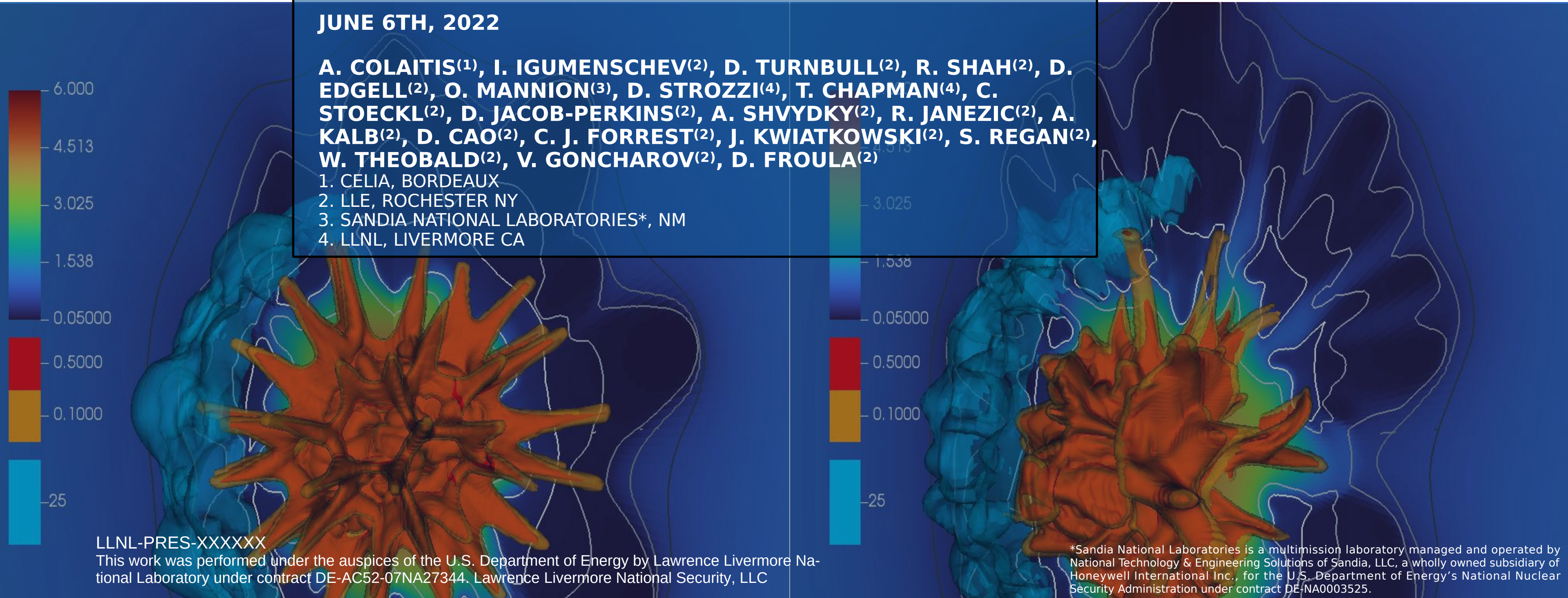

LLNL-PRES-XXXXXX
This work was performed under the auspices of the U.S. Department of Energy by Lawrence Livermore National Laboratory under contract DE-AC52-07NA27344. Lawrence Livermore National Security, LLC

*Sandia National Laboratories is a multimission laboratory managed and operated by National Technology & Engineering Solutions of Sandia, LLC, a wholly owned subsidiary of Honeywell International Inc., for the U.S. Department of Energy's National Nuclear Security Administration under contract DE-NA0003525.

DIRECT-DRIVE ICF RELIES ON HIGH LEVELS OF SYMMETRY TO REACH HIGH GAINS, WHICH ARE NECESSARY FOR ENERGY PRODUCTION

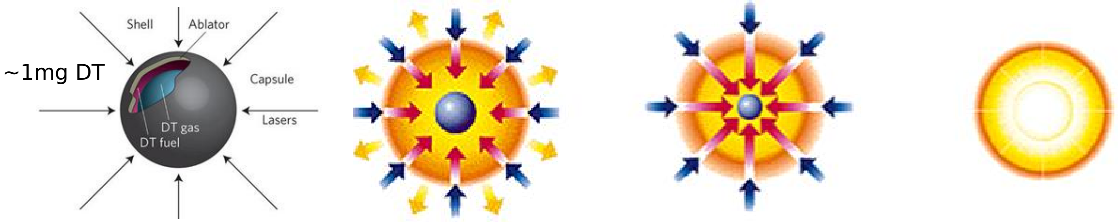

heating *implosion* *ignition* *burn*

DIRECT-DRIVE ICF RELIES ON HIGH LEVELS OF SYMMETRY TO REACH HIGH GAINS, WHICH ARE NECESSARY FOR ENERGY PRODUCTION

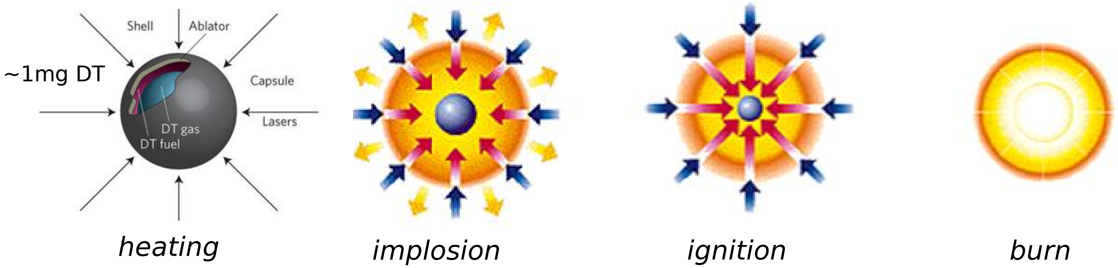

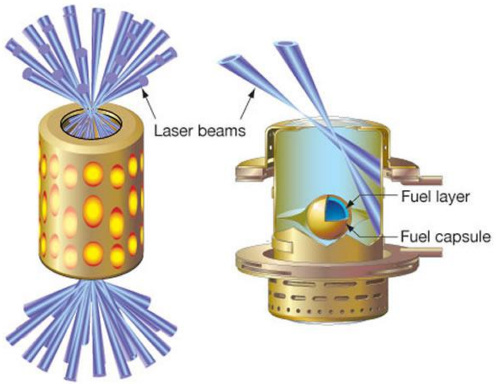

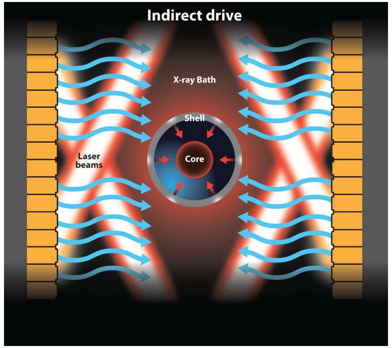

Indirect-drive approach

- Lower gain (X-ray conversion)
- Higher drive smoothness
- Time-dependant cylindrical drive to implode a spherical capsule

DIRECT-DRIVE ICF RELIES ON HIGH LEVELS OF SYMMETRY TO REACH HIGH GAINS, WHICH ARE NECESSARY FOR ENERGY PRODUCTION

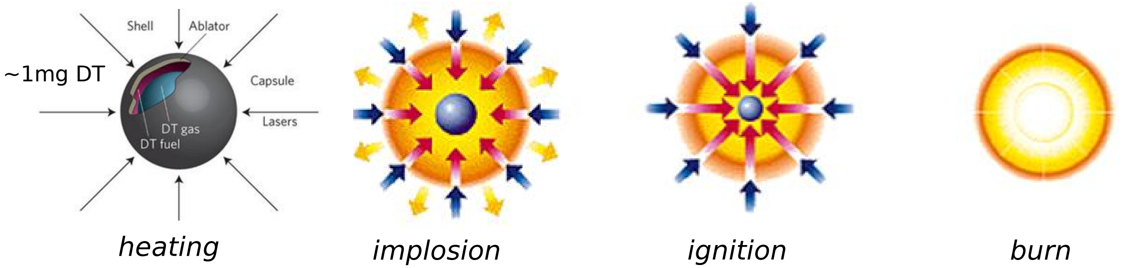

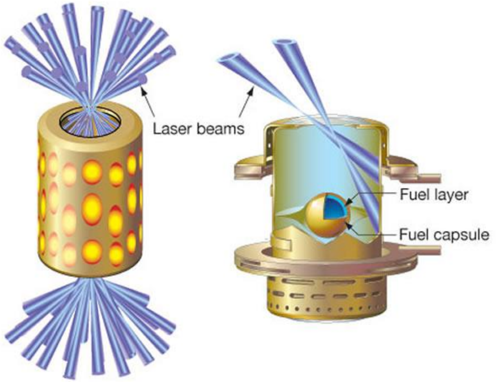

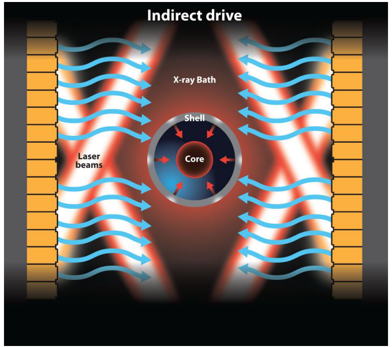

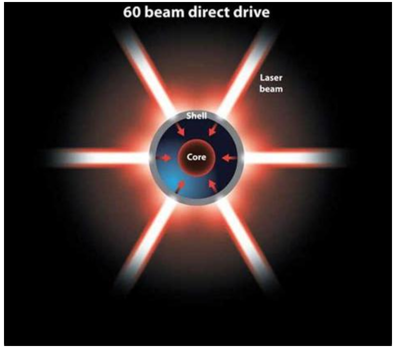

Indirect-drive approach
- Lower gain (X-ray conversion)
- Higher drive smoothness
- Time-dependant cylindrical drive to implode a spherical capsule

Direct-drive approach => favored for energy production
- Higher gain
- More sensitive to 3D laser effects (imbalance, alignment, etc) and beam smoothness

Understanding the sources of implosion perturbations is key to reach high gains for inertial fusion energy

BEST-SETUP EXPERIMENTS ON OMEGA IN 2019-2020 EXHIBIT SYSTEMATIC FLOW ANOMALIES

Database of 111 shots conducted in 2019-2020 on OMEGA
=> down-selection of 12 shots with:

- 60 beams, full SSD
- good ice thickness uniformity (<1% l=1)
- good ice surface roughness
- low pointing error (<2% l=1, <2% l=2   to <1% l =1)
- low power imbalance
- low target offset (< 5 microns to < 1 micron)

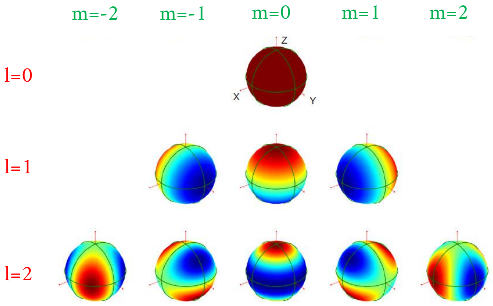

BEST-SETUP EXPERIMENTS ON OMEGA IN 2019-2020 EXHIBIT SYSTEMATIC FLOW ANOMALIES

Database of 111 shots conducted in 2019-2020 on OMEGA
=> down-selection of 12 shots with:
- 60 beams, full SSD
- good ice thickness uniformity (<1% l=1)
- good ice surface roughness
- low pointing error (<2% l=1, <2% l=2   to <1% l =1)
- low power imbalance
- low target offset (< 5 microns to < 1 micron)

… there remain a significant mode 1 assymetry in the DT flow at stagnation, that does not seem correlated to mispointing error, cryo/warm, or shot-day anomalies

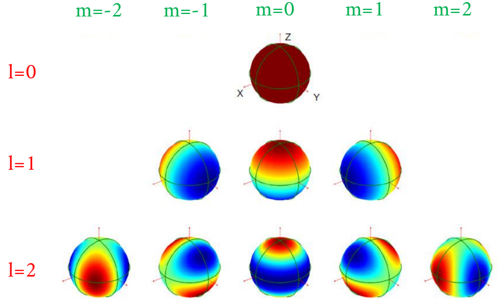

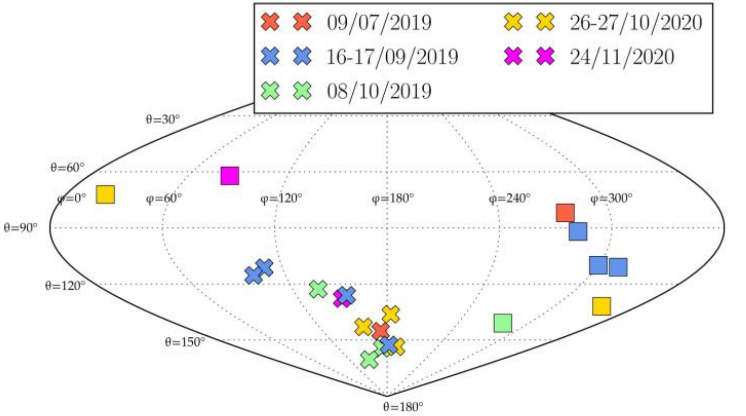

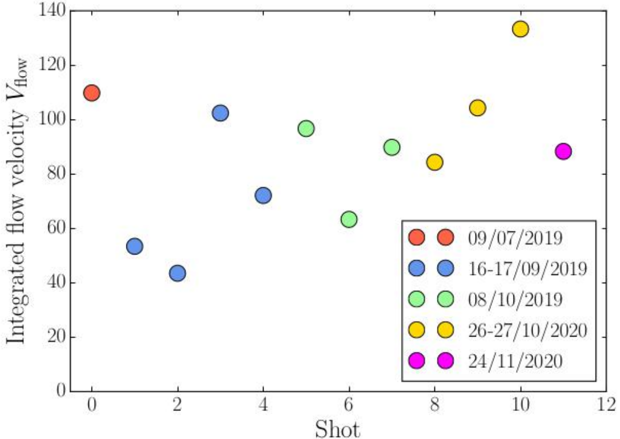

BEST-SETUP EXPERIMENTS ON OMEGA IN 2019-2020 EXHIBIT SYSTEMATIC FLOW ANOMALIES

Database of 111 shots conducted in 2019-2020 on OMEGA
=> down-selection of 12 shots with:
- 60 beams, full SSD
- good ice thickness uniformity (<1% l=1)
- good ice surface roughness
- low pointing error (<2% l=1, <2% l=2 to <1% l =1)
- low power imbalance
- low target offset (< 5 microns to < 1 micron)

... there remain a significant mode 1 assymetry in the DT flow at stagnation, that does not seem correlated to mispointing error, cryo/warm, or shot-day anomalies

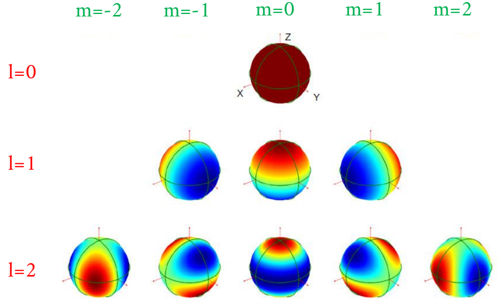

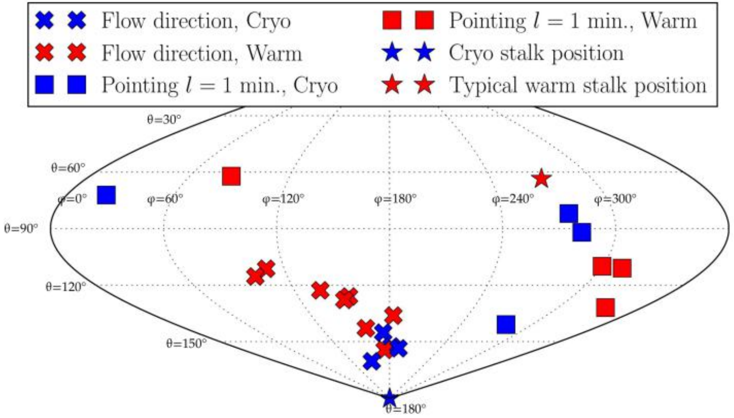

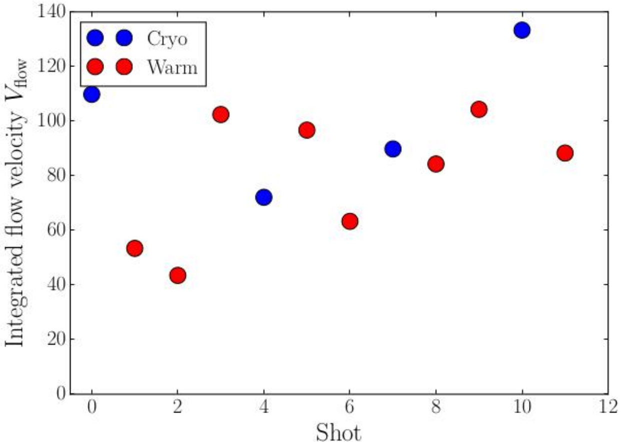

BEST-SETUP EXPERIMENTS ON OMEGA IN 2019-2020 EXHIBIT SYSTEMATIC FLOW ANOMALIES

Database of 111 shots conducted in 2019-2020 on OMEGA
=> down-selection of 12 shots with:

- 60 beams, full SSD
- good ice thickness uniformity (<1% l=1)
- good ice surface roughness
- low pointing error (<2% l=1, <2% l=2 to <1% l =1)
- low power imbalance
- low target offset (< 5 microns to < 1 micron)

… there remain a significant mode 1 assymetry in the DT flow at stagnation, that does not seem correlated to mispointing error, cryo/warm, or shot-day anomalies

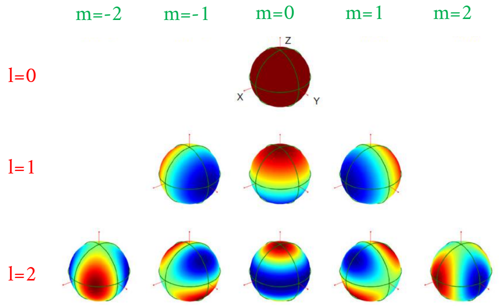

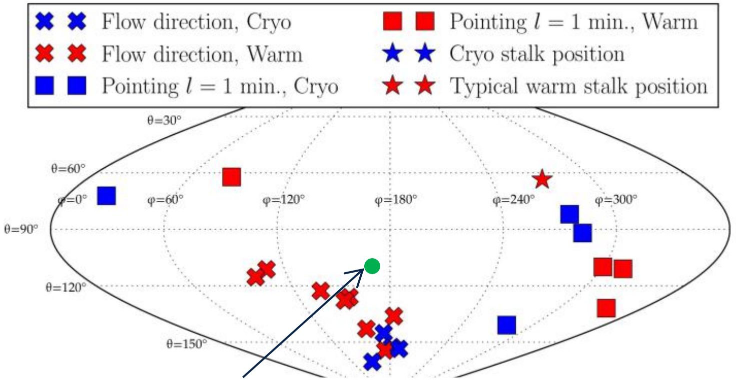

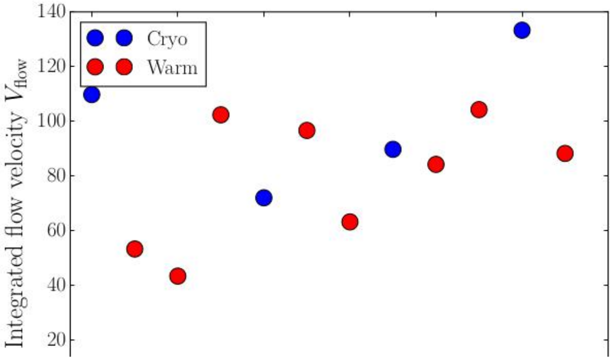

Low mode direction from offline calculation of CBET polarization effect [D. Edgell et al. PRL (2022)]

OUTLINE

- Is the polarization effect of CBET responsible for the systematic anomaly ?
- If including most sources of low modes, can the modeling reproduce the OMEGA measurements for neutron data ? (is the modeling also accurate at NIF scale ?)
- What is the relative contribution of these sources to yield degradation ?
- How to mitigate low modes ?
- Polarization anomaly on NIF ?

UNPOLARIZED CBET FROM A SYMMETRIC BEAM PATTERN PRODUCES A SYMMETRIC IRRADIATION

Why would the polarization effect matter … ?

Cross Beam Energy Transfer (CBET) transfers energy between beams through a shared IAW grating

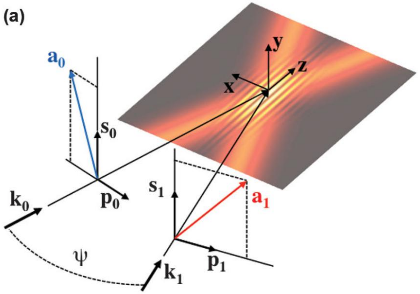

[P. Michel et al. PoP 17 (2010)]

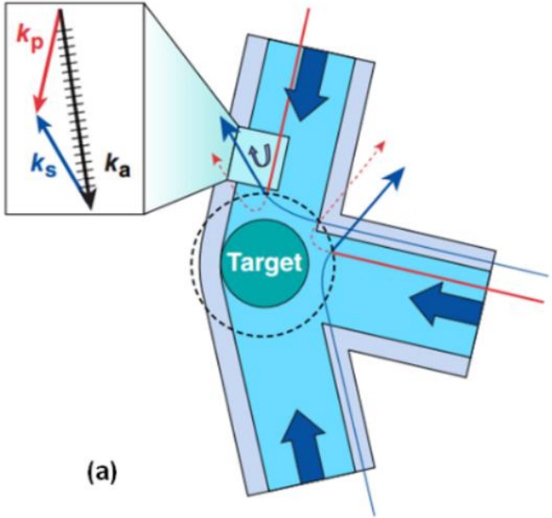

[A. K. Davis et al. PoP (2016)]

In direct-drive, reflected beams “steal” energy from incident beams

If the laser configuration is **perfectly symetric**, the unpolarized CBET also remains symmetric

POLARIZATION EFFECTS CONTRIBUTE TO THE DETAILS OF CBET AMPLIFICATION

Why would the polarization effect matter … ?

- Ellipticity induced from propagation in a bi-refringent medium formed by the IAW grating
- Probe beam polarization rotation toward that of the pump
- Polarization transport through refraction

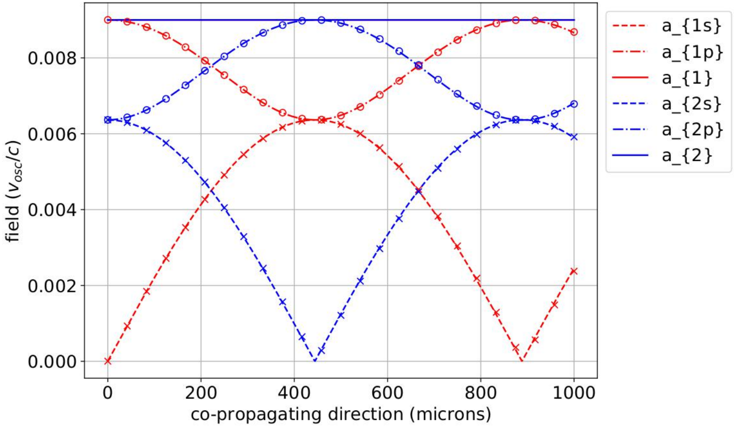

Beams interacting in a medim with $\mathrm{Im}(K) = 0$ and $\mathrm{Re}(K) \neq 0$

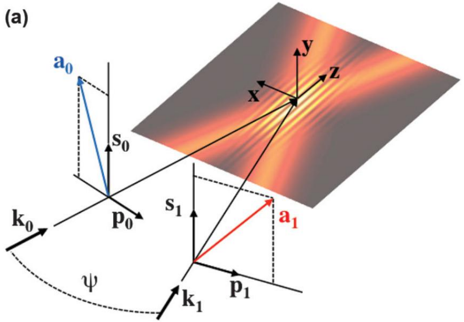

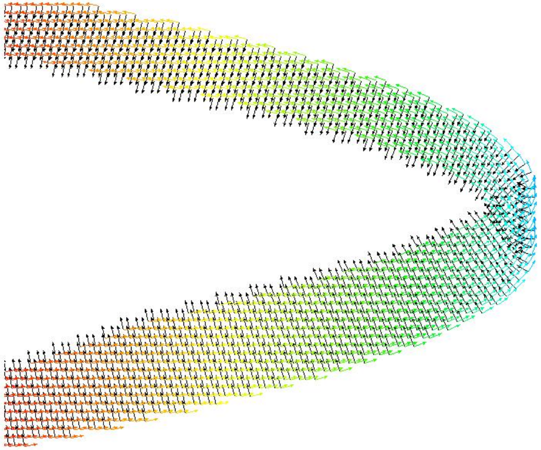

THE POLARIZATION CONFIGURATION ON OMEGA IS NON-SYMMETRIC

Why would the polarization effect matter … ?

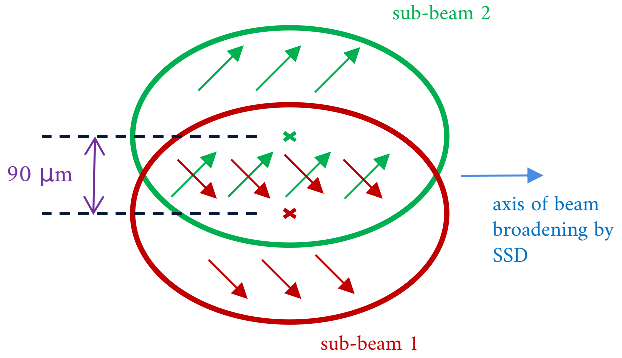

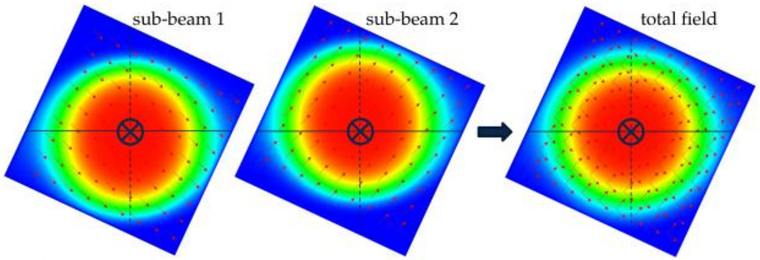

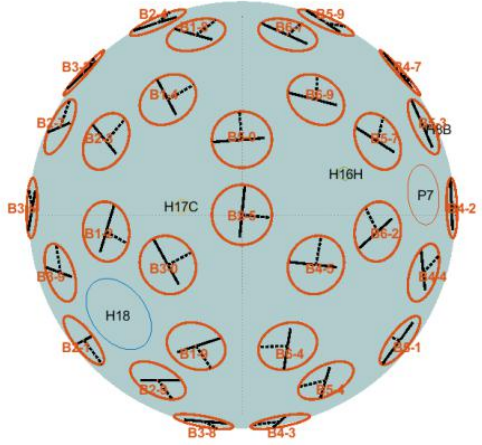

Distributed Polarization Rotators introduce a preferential axis that breaks the spherical symmetry

INLINE MODELING OF POLARIZED CBET RELIES ON DECOMPOSITION OF THE FIELD ON THE FRENET FRAME OF RAYS

Frenet reference frame

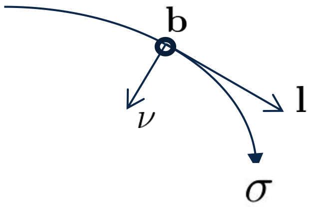

$$\boldsymbol{\nu} = \frac{1}{2\mathcal{K}\epsilon'}\nabla_\perp \epsilon'$$

$$\mathcal{K} = \frac{1}{2}\left|\frac{\nabla\epsilon'}{\epsilon'}\times \mathbf{l}\right|$$

$$\frac{\mathrm{d}\boldsymbol{\nu}}{\mathrm{d}\sigma} = -\mathcal{K}\mathbf{l} + \kappa\mathbf{b}$$

$$\kappa = \cancelto{0}{\mathbf{b}.\frac{\mathrm{d}\boldsymbol{\nu}}{\mathrm{d}\sigma}}$$

INLINE MODELING OF POLARIZED CBET RELIES ON DECOMPOSITION OF THE FIELD ON THE FRENET FRAME OF RAYS

Frenet reference frame

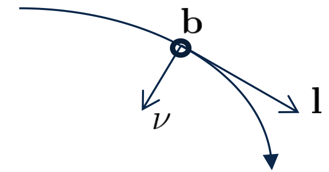

$$\boldsymbol{\nu} = \frac{1}{2\mathcal{K}\epsilon'}\nabla_\perp \epsilon'$$

$$\mathcal{K} = \frac{1}{2}\left|\frac{\nabla\epsilon'}{\epsilon'} \times \mathbf{l}\right|$$

$$\frac{\mathrm{d}\boldsymbol{\nu}}{\mathrm{d}\sigma} = -\mathcal{K}\mathbf{l} + \kappa\mathbf{b}$$

$$\kappa = \mathbf{b}.\cancelto{0}{\frac{\mathrm{d}\boldsymbol{\nu}}{\mathrm{d}\sigma}}$$

$$\frac{\partial \mathbf{a}_1}{\partial \mathbf{l}_1} = \frac{\imath}{8k_1} K_{10} k_{b,10}^2 (\mathbf{a}_0^\star . \mathbf{a}_1)\mathbf{a}_0$$

$$\frac{\partial \mathbf{a}_0}{\partial \mathbf{l}_0} = \frac{\imath}{8k_0} K_{01} k_{b,01}^2 (\mathbf{a}_0 . \mathbf{a}_1^\star)\mathbf{a}_1$$

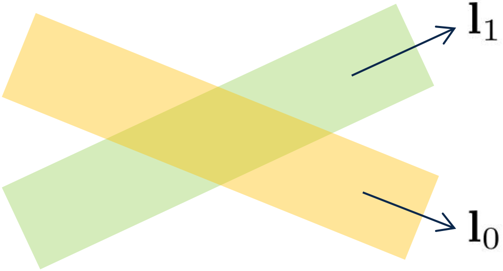

Coupling eqs. between 3D complex fields

INLINE MODELING OF POLARIZED CBET RELIES ON DECOMPOSITION OF THE FIELD ON THE FRENET FRAME OF RAYS

Frenet reference frame

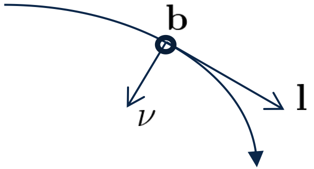

$$\boldsymbol{\nu} = \frac{1}{2\mathcal{K}\epsilon'}\nabla_{\perp}\epsilon'$$

$$\mathcal{K} = \frac{1}{2}\left|\frac{\nabla\epsilon'}{\epsilon'} \times \mathbf{l}\right|$$

$$\frac{\mathrm{d}\boldsymbol{\nu}}{\mathrm{d}\sigma} = -\mathcal{K}\mathbf{l} + \kappa\mathbf{b}$$

$$\kappa = \mathbf{b}.\cancelto{0}{\frac{\mathrm{d}\boldsymbol{\nu}}{\mathrm{d}\sigma}}$$

Complex s/p components in the Frenet frame

$$\frac{\partial}{\partial \mathbf{l}_n}\begin{pmatrix} a_{n,\nu_n} \\ a_{n,b_n} \end{pmatrix} = \underline{\underline{\mathcal{D}_n}}\cdot\begin{pmatrix} a_{n,\nu_n} \\ a_{n,b_n} \end{pmatrix}$$

$$\frac{\partial \mathbf{a}_1}{\partial \mathbf{l}_1} = \frac{\imath}{8k_1}K_{10}k_{b,10}^2(\mathbf{a}_0^{\star}.\mathbf{a}_1)\mathbf{a}_0$$

$$\frac{\partial \mathbf{a}_0}{\partial \mathbf{l}_0} = \frac{\imath}{8k_0}K_{01}k_{b,01}^2(\mathbf{a}_0.\mathbf{a}_1^{\star})\mathbf{a}_1$$

$$\longrightarrow \quad \underline{\underline{\mathcal{D}_n}} = \frac{\imath}{8k_n}\sum_{\substack{m\in\text{beams,sheets}\\ m\neq n}}^{N} K_{nm}^{\star}k_{b,nm}^2\underline{\underline{\mathbf{M_{nm}}}}$$

Complex kinetic plasma response
Langdon and Dewandre effect
Real part: induces ellipticity
Imaginary part: depletion or gain

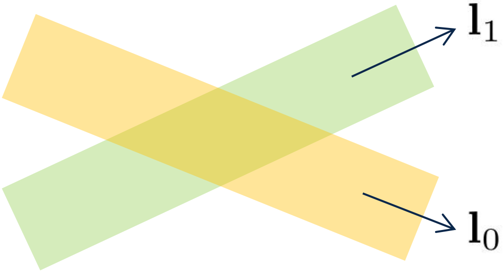

Coupling eqs. between 3D complex fields

INLINE MODELING OF POLARIZED CBET RELIES ON DECOMPOSITION OF THE FIELD ON THE FRENET FRAME OF RAYS

Frenet reference frame

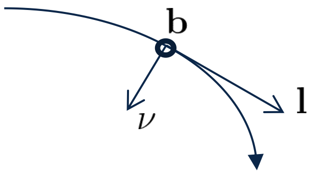

$$\boldsymbol{\nu} = \frac{1}{2\mathcal{K}\epsilon'}\nabla_\perp \epsilon'$$

$$\mathcal{K} = \frac{1}{2}\left|\frac{\nabla\epsilon'}{\epsilon'} \times \mathbf{l}\right|$$

$$\frac{\mathrm{d}\boldsymbol{\nu}}{\mathrm{d}\sigma} = -\mathcal{K}\mathbf{l} + \kappa\mathbf{b}$$

$$\kappa = \mathbf{b}.\cancelto{0}{\frac{\mathrm{d}\boldsymbol{\nu}}{\mathrm{d}\sigma}}$$

Complex s/p components in the Frenet frame

$$\frac{\partial}{\partial \mathbf{l}_n}\begin{pmatrix} a_{n,\nu_n} \\ a_{n,b_n} \end{pmatrix} = \underline{\underline{\mathcal{D}_n}}.\begin{pmatrix} a_{n,\nu_n} \\ a_{n,b_n} \end{pmatrix}$$

$$\frac{\partial \mathbf{a}_1}{\partial \mathbf{l}_1} = \frac{\imath}{8k_1} K_{10} k_{b,10}^2 (\mathbf{a}_0^\star . \mathbf{a}_1)\mathbf{a}_0$$

$$\frac{\partial \mathbf{a}_0}{\partial \mathbf{l}_0} = \frac{\imath}{8k_0} K_{01} k_{b,01}^2 (\mathbf{a}_0 . \mathbf{a}_1^\star)\mathbf{a}_1$$

$$\longrightarrow$$

$$\underline{\underline{\mathcal{D}_n}} = \frac{\imath}{8k_n} \sum_{\substack{m \in \text{beams,sheets} \\ m \neq n}}^{N} K_{nm}^\star k_{b,nm}^2 \underline{\underline{\mathbf{M_{nm}}}}$$

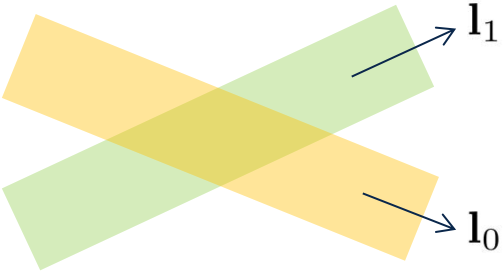

$$\underline{\underline{\mathbf{M_{nm}}}} = \begin{pmatrix} \boxed{a_{m,\nu_n}^2} & a_{m,b_n}^\star a_{m,\nu_n} \\ a_{m,b_n} a_{m,\nu_n}^\star & a_{m,b_n}^2 \end{pmatrix}$$

Matrix responsible for polarization rotation and ellipticity

"Usual" coupling

$$\begin{pmatrix} \epsilon_{i,j,\nu_n} \\ \epsilon_{i,j,b_n} \end{pmatrix} = [\epsilon_i' + \imath(\epsilon_{0,i}'' f_{\mathrm{L}} + \underline{\underline{\mathcal{D}_{i,j}}})].\begin{pmatrix} 1 \\ 1 \end{pmatrix}$$

Coupling eqs. between 3D complex fields

Each polarization component sees a different permittivity

INLINE MODELING OF POLARIZED CBET RELIES ON DECOMPOSITION OF THE FIELD ON THE FRENET FRAME OF RAYS

Frenet reference frame

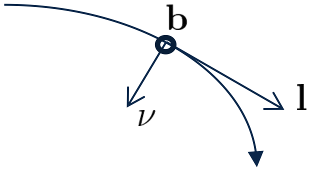

$$\boldsymbol{\nu} = \frac{1}{2\mathcal{K}\epsilon'}\nabla_\perp \epsilon'$$

$$\mathcal{K} = \frac{1}{2}\left|\frac{\nabla\epsilon'}{\epsilon'} \times \mathbf{l}\right|$$

$$\frac{d\boldsymbol{\nu}}{d\sigma} = -\mathcal{K}\mathbf{l} + \kappa\mathbf{b}$$

$$\kappa = \mathbf{b}.\cancelto{0}{\frac{d\boldsymbol{\nu}}{d\sigma}}$$

Complex s/p components in the Frenet frame

$$\frac{\partial \mathbf{a}_1}{\partial \mathbf{l}_1} = \frac{\imath}{8k_1} K_{10} k_{b,10}^2 (\mathbf{a}_0^\star . \mathbf{a}_1)\mathbf{a}_0$$

$$\frac{\partial \mathbf{a}_0}{\partial \mathbf{l}_0} = \frac{\imath}{8k_0} K_{01} k_{b,01}^2 (\mathbf{a}_0 . \mathbf{a}_1^\star)\mathbf{a}_1$$

→

$$\frac{\partial}{\partial \mathbf{l}_n}\begin{pmatrix} a_{n,\nu_n} \\ a_{n,b_n} \end{pmatrix} = \underline{\underline{\mathcal{D}_n}}.\begin{pmatrix} a_{n,\nu_n} \\ a_{n,b_n} \end{pmatrix}$$

$$\underline{\underline{\mathcal{D}_n}} = \frac{\imath}{8k_n}\sum_{\substack{m\in\text{beams,sheets}\\ m\neq n}}^{N} K_{nm}^\star k_{b,nm}^2 \underline{\underline{\mathbf{M_{nm}}}}$$

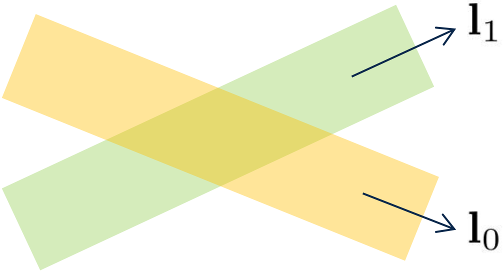

Coupling eqs. between 3D complex fields

$$\underline{\underline{\mathbf{M_{nm}}}} = \begin{pmatrix} a_{m,\nu_n}^2 & a_{m,b_n}^\star a_{m,\nu_n} \\ a_{m,b_n} a_{m,\nu_n}^\star & a_{m,b_n}^2 \end{pmatrix}$$

Matrix responsible for polarization rotation and ellipticity

“Usual” coupling

The Polarized model requires 8x more computations than the standard “unpolarized” model (2 DPR components x 2 polarization components x 2 {real + imaginary})

THE UNPOLARIZED CBET ON OMEGA INDUCES NO SIGNIFICANT ASSYMETRY ON THE ENERGY DEPOSITION

Heat source calculated in a 1D hydro profile - no CBET

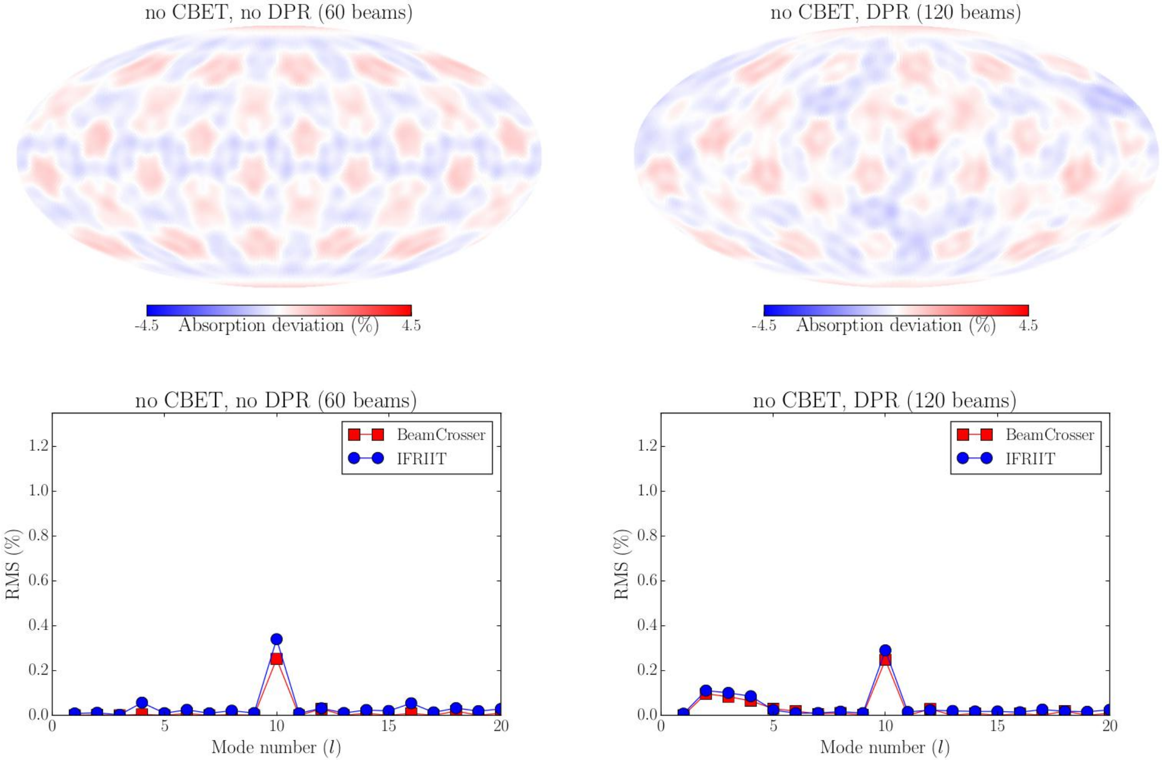

The DPR system itself induces slight low modes, small effect

THE POLARIZED CBET INDUCES A NON-NEGLIGIBLE LOW MODE ANOMALY ON THE ENERGY DEPOSITION PATTERN

Heat source calculated in a 1D hydro profile - CBET

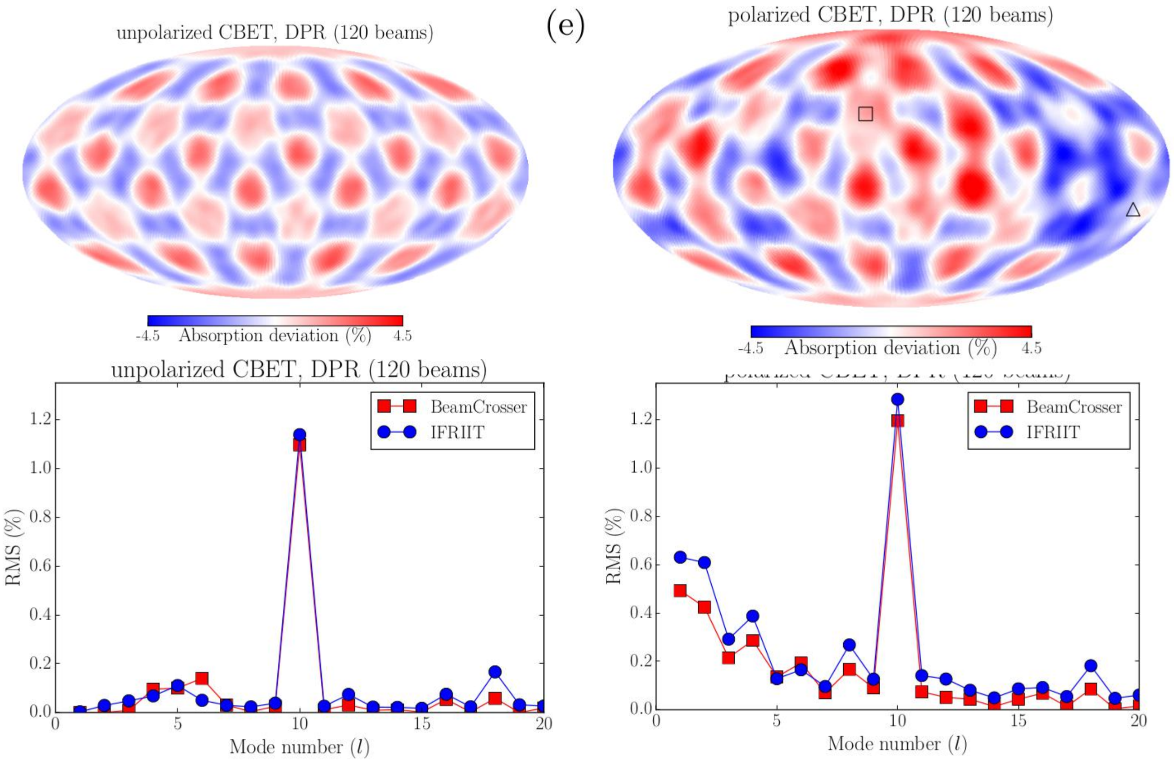

The polarization effect induces significant low modes
Consistent with results from D. Edgell obtained using BeamletCrosser postprocessor
What is the compound effect accounting for hydrodynamics feedback and other low mode sources ?

THE ASTER+IFRIIT COUPLED CODE WAS DEVELOPPED TO STUDY ICF IMPLOSIONS CONSIDERING MOST LOW MODE SOURCES

ASTER+IFRIIT code coupling

[A. Colaïtis, I. V. Igumenshchev et al. JCP (2021)]

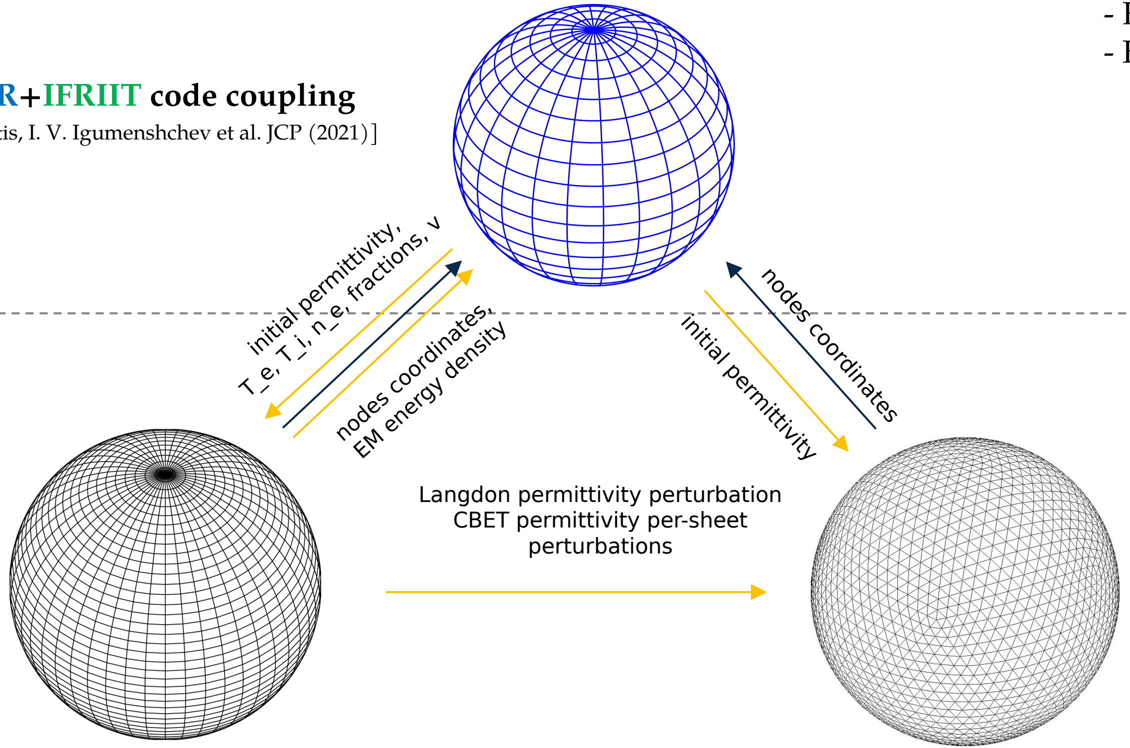

aster mesh
typical size: 20-500M nodes

initial permittivity,
T_e, T_i, n_e, fractions, v

nodes coordinates,
EM energy density

nodes coordinates

initial permittivity

Langdon permittivity perturbation
CBET permittivity per-sheet
perturbations

observation mesh
typical size: 0.5-1.5M nodes

raytracing mesh
typical size: 1-10M nodes, 5-50M tetras

ASTER 3-D radiative hydrodynamics code

- Eulerian spherical moving grid
- EOS, heat transport, radiation, hydro...
- High resolution, block-decomposed MPI

[I. V. Igumenshchev et al. PoP (2016),
I. V. Igumenshchev et al. PoP (2017)]

IFRIIT 3-D laser propagation code

- Inverse Ray Tracing for fast and low noise field computations
- Caustic modeling with Etalon Integrals
- CBET with many physics models, including polarization
- Adaptive resolution, domain-duplicated MPI/OpenMP

[A. Colaïtis et al., PoP 26(3) (2019),
A. Colaïtis et al., PoP 26(7) (2019)]

WE STUDY 4 SHOTS CONSIDERING MOST LOW MODE SOURCES

Shot number	Date	Type	E_{las} (kJ)	D_t (μm)	Offset magnitude (μm)	Pointing shot	Pointing $l = 1$ (% RMS)	Balance $l = 1$ (% RMS) picket	early drive	late drive
94343	09/07/2019	cryo	27.7	982	3.5	94336	1.26	2.58	0.48	1.45
94712	09/08/2019	cryo	28.4	961.4	7.0*	94708	5.94	4.52	0.35	1.34
98768	27/10/2020	cryo	28.4	1012	3.2	98762	1.08	1.72	0.43	1.7
98755	26/10/2020	warm	27.9	978.2	1.3	98754/98757	0.64/1.0	0.71	0.79	0.92

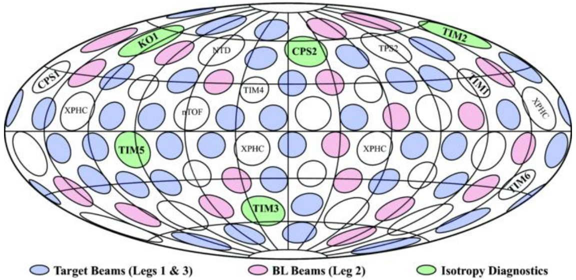

OMEGA detailed beam geometry
120 DPR-split beams

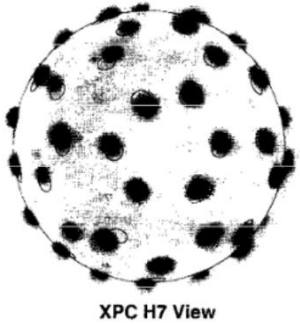

Measured beam pointing (from begining and/or end of shot day)

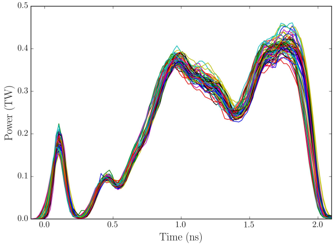

Measured pulse shapes

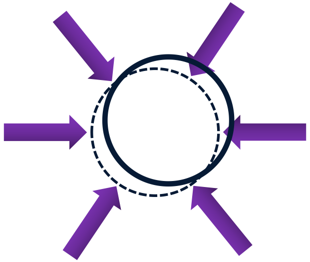

Measured offset (if available)

Important note: contrary to most inline approaches, the CBET model here has no "ad-hoc" parameter => thanks to the caustic modeling. No IAW saturation is assumed.

THE 3D MODELING REPRODUCES THE EXPERIMENTALLY MEASURED BANG TIME AND NEUTRON YIELD

Simulation results presented for 4 shots are studied ; 3 cryogenic and one « warm » shot
Total ~ 60M CPU hours of computation

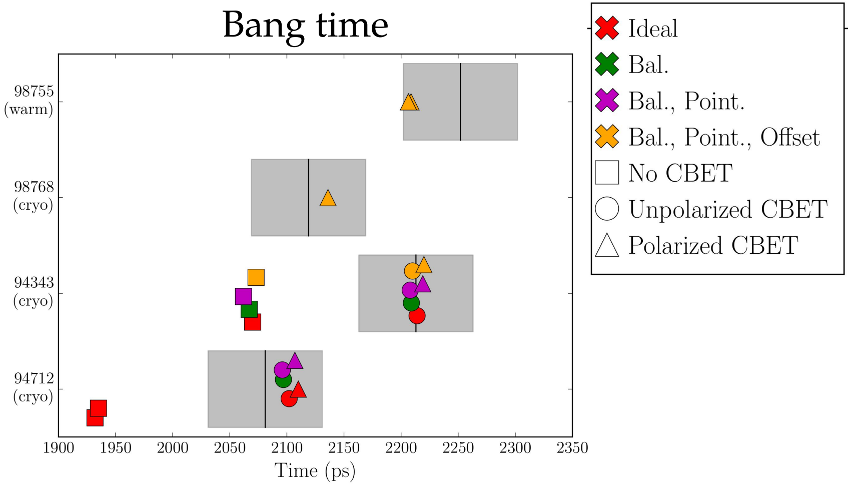

THE 3D MODELING REPRODUCES THE EXPERIMENTALLY MEASURED BANG TIME AND NEUTRON YIELD

Simulation results presented for 4 shots are studied ; 3 cryogenic and one « warm » shot
Total ~ 60M CPU hours of computation

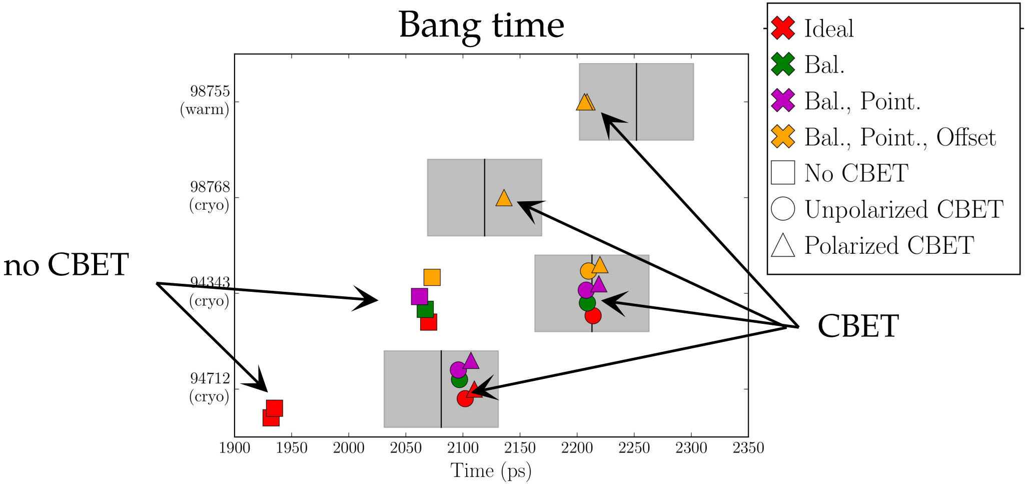

(i) The CBET model alone gets the nuclear bang time correct (drive energetics is well modeled)

THE 3D MODELING REPRODUCES THE EXPERIMENTALLY MEASURED BANG TIME AND NEUTRON YIELD

Simulation results presented for 4 shots are studied ; 3 cryogenic and one « warm » shot
Total ~ 60M CPU hours of computation

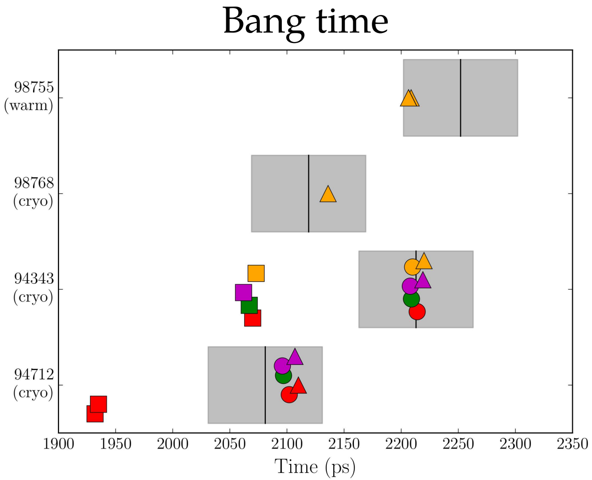
Bang time

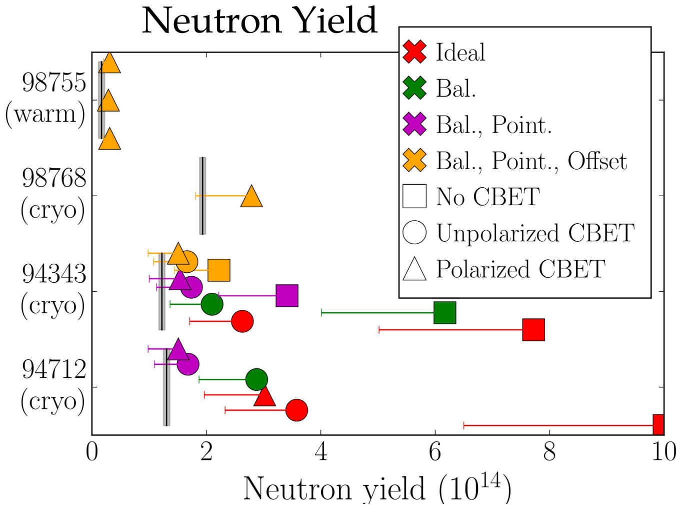
Neutron Yield

(i) The CBET model alone gets the nuclear bang time correct (drive energetics is well modeled)
(ii) CBET simulations with power balanace and pointing variation get the neutron yield correctly because both drive energetics and symmetry are important to the yield

Note:

- experimental yields are corrected for fuel aging (tritium decay, 3He contamination and radiological capsule damage)

THE 3D MODELING REPRODUCES THE EXPERIMENTALLY MEASURED BANG TIME AND NEUTRON YIELD

Simulation results presented for 4 shots are studied ; 3 cryogenic and one « warm » shot
Total ~ 60M CPU hours of computation

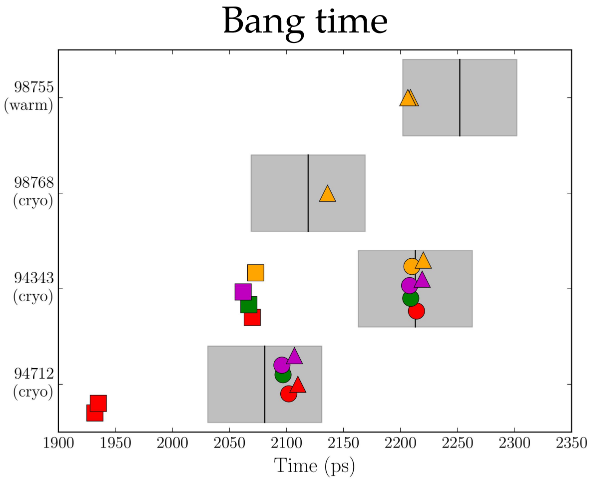

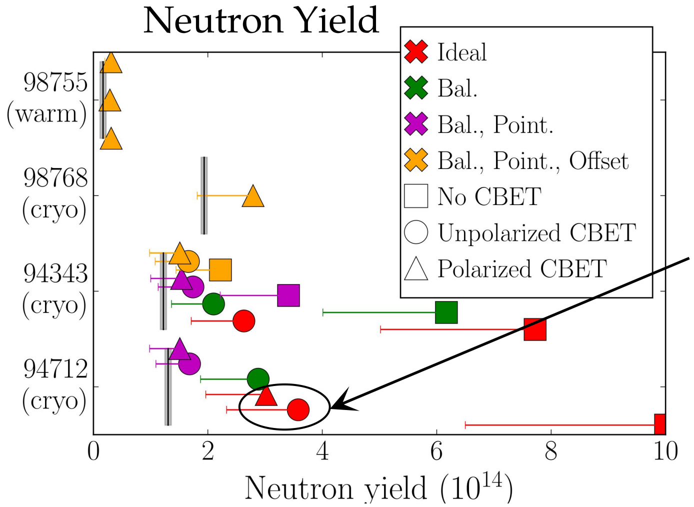

Polarization alone causes a 15% yield drop

(i) The CBET model alone gets the nuclear bang time correct (drive energetics is well modeled)
(ii) CBET simulations with power balanace and pointing variation get the neutron yield correctly because both drive energetics and symmetry are important to the yield

Note:
- experimental yields are corrected for fuel aging (tritium decay, 3He contamination and radiological capsule damage)

THE 3D MODELING ALSO APPROACHES WELL THE FLOW VELOCITY MAGNITUDE AND DIRECTION

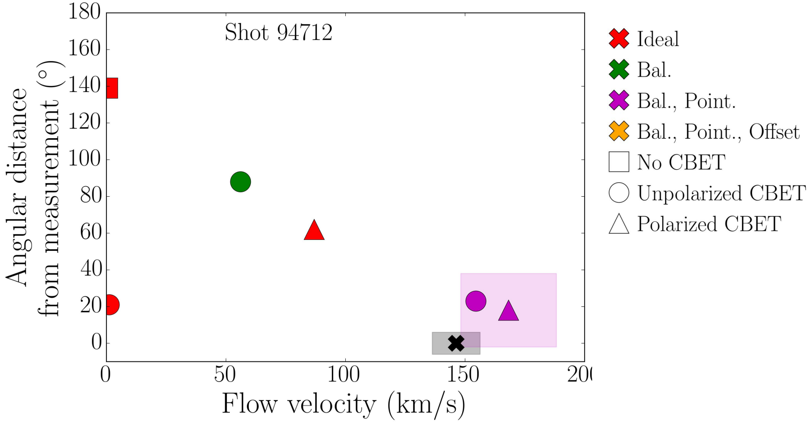

(iii) CBET with power balance and pointing variations match the flow velocity vector for 94712 because the large pointing error dominates the low mode sources

THE 3D MODELING ALSO APPROACHES WELL THE FLOW VELOCITY MAGNITUDE AND DIRECTION

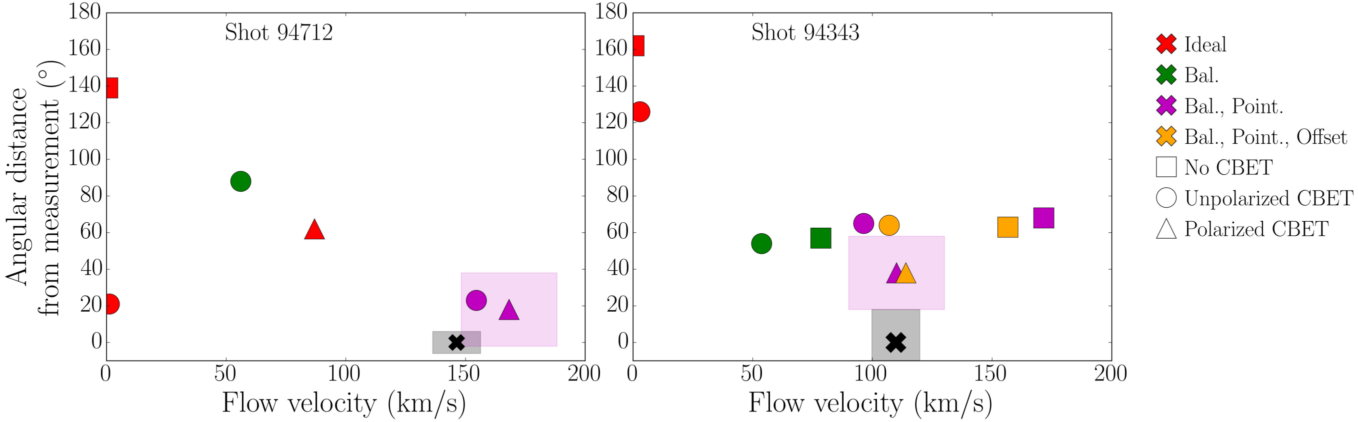

(iii) CBET with power balance and pointing variations match the flow velocity vector for 94712 because the large pointing error dominates the low mode sources

(iv) Polarized CBET with power balance and pointing is needed to get the flow velocity correctly for the more accurately pointed shot 94343 => the polarization effect begins to be more important as other low mode sources become smaller

THE 3D MODELING ALSO APPROACHES WELL THE FLOW VELOCITY MAGNITUDE AND DIRECTION

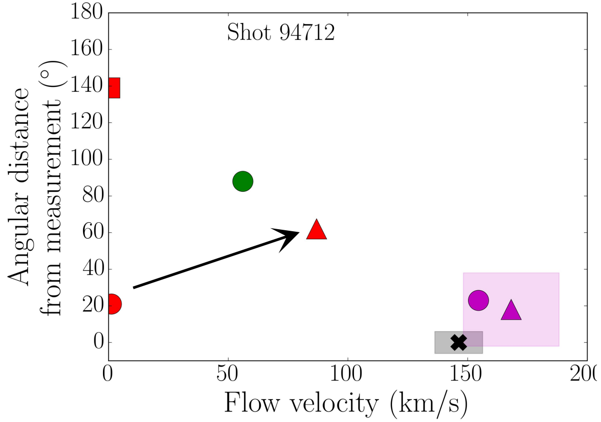

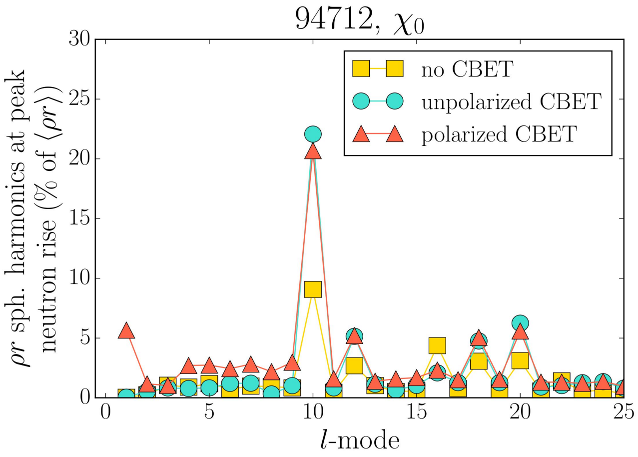

(iii) CBET with power balance and pointing variations match the flow velocity vector for 94712 because the large pointing error dominates the low mode sources
(iv) Polarized CBET with power balance and pointing is needed to get the flow velocity correctly for the more accurately pointed shot 94343 => the polarization effect begins to be more important as other low mode sources become smaller

Note the single effect of polarized CBET, that induces a ~80 km/s flow in the ideal case

THE MODELING SYSTEMATICALLY APPROACHES THE MEASURED FLOW DIRECTION

Good agreement in flow direction also for 98768

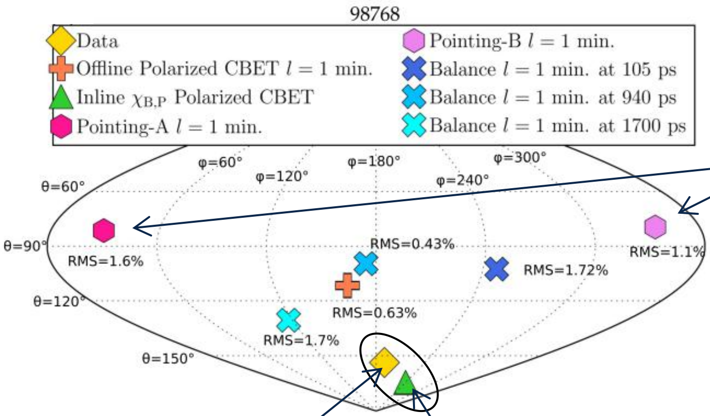

Note: 53° between two pointing analysis of the same pointing shot

For this shot, the simulation underestimates the flow velocity (72 km/s vs 133 km/s measured)

Data

Simulation

THE KNOWLEDGE OF THE ACTUAL POINTING MODES IS LIMITING OUR AGREEMENT WITH THE DATA

Note:

- 80 to 100° difference between the morning and afternoon pointing shots despite no TIM transaction

For this shot, the simulations underestimates the flow velocity (50 km/s vs 84 km/s measured)

=> Knowledge of pointing limitates our predictability of flow direction

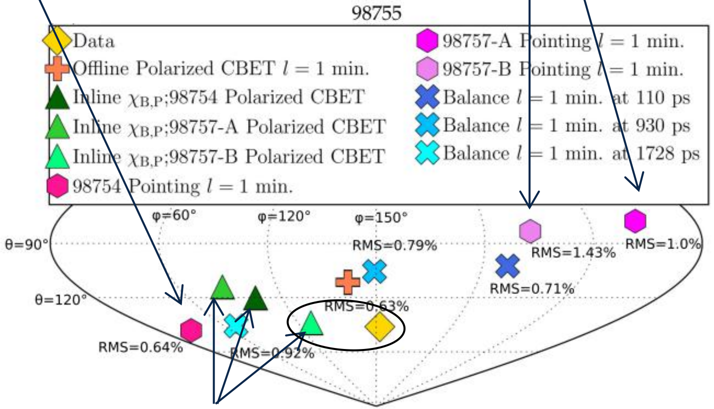

Afternoon pointing shot

Morning pointing shot

Three simulations with three pointings

THE CURRENT BEST PERFORMANCES OF THE LASER SYSTEM CAN STILL CAUSE HIGHLY SIGNIFICANT FLOW ANOMALIES

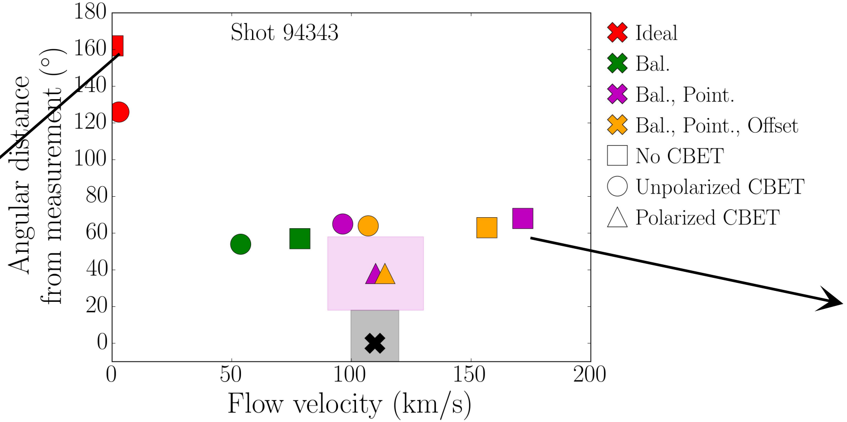

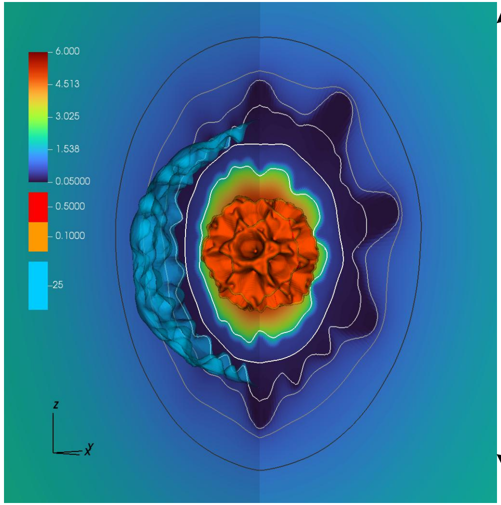

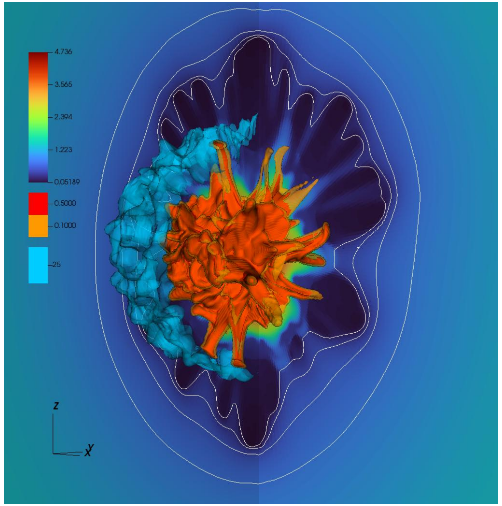

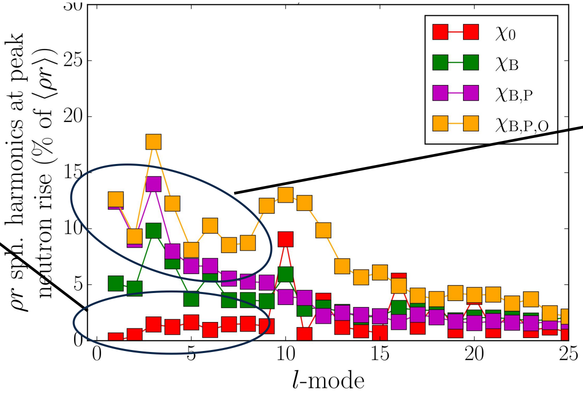

Without CBET, best levels of pointings, balance and offset introduce significant low modes at stagnation, with **DT flows that can reach up to 170 km/s**

THE CURRENT BEST PERFORMANCES OF THE LASER SYSTEM CAN STILL CAUSE HIGHLY SIGNIFICANT FLOW ANOMALIES

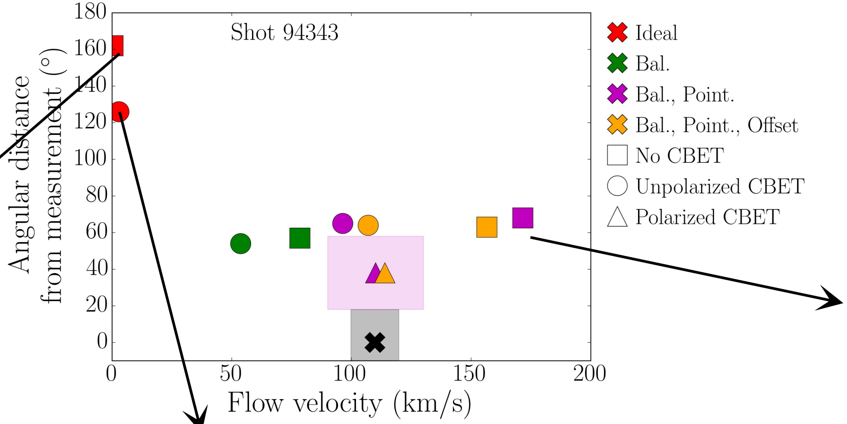

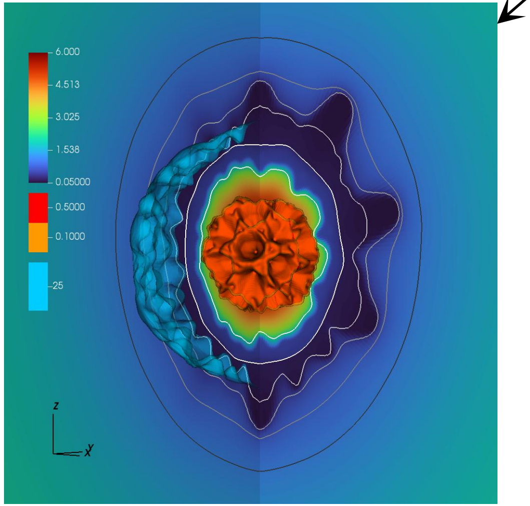

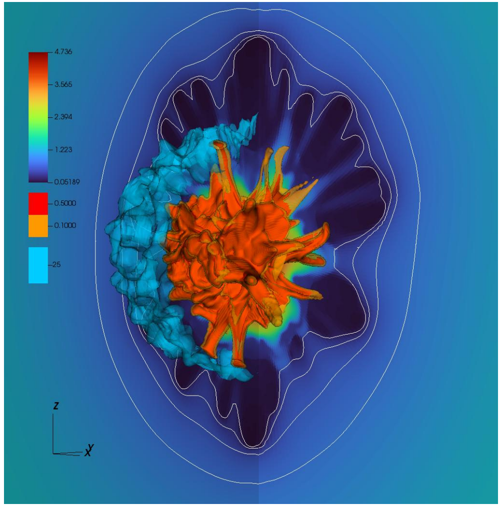

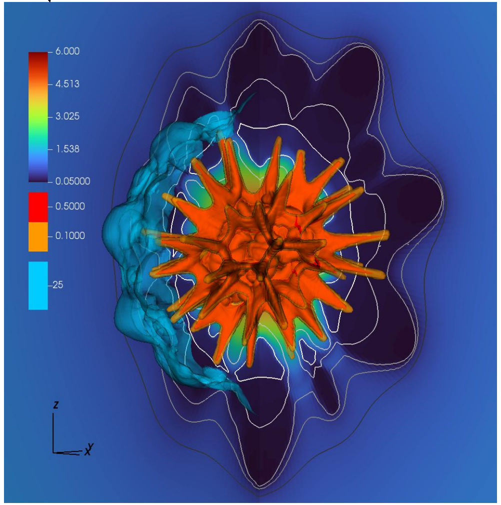

In ideal conditions, CBET amplifies mode 10 sufficiently to lead to target perforation

TOTAL ENERGY COUPLING IS STRONGLY DRIVEN BY CBET AND SYSTEM LOW MODES

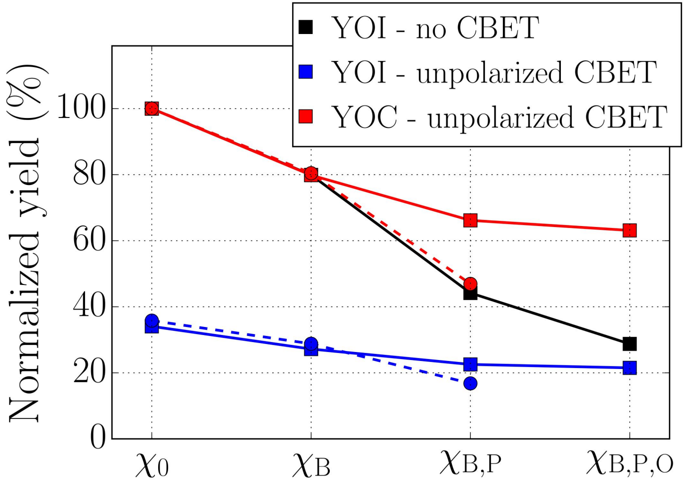

solid: 94343
dashed: 94712

- **CBET** alone **reduces neutron yields by ~60 %** in the ideal case → a realistic fusion driver must remove CBET
- **System-induced low modes are mitigated by CBET** → designs without CBET must be made more robust to low modes

=> How to mitigate low modes ? We can explore two mitigation strategies (current and envisonned)

MITIGATION OF LOW MODES BY TARGET OFFSET CAN ONLY RECOVER A FINITE AMOUNT OF YIELD

Strategy 1 : offset mitigation

- In experiments, the target can be offset opposite to the direction of the measured flow anomaly (this is used routinely to improve yields)

Pros : Simple to implement, allows to recover ~15 % in yield at maximum here

Cons : The method rapidly reaches a maximum efficacy due to it mitigating only l=1. In particular, even in the ideal case, polarized CBET introduces other modes than l=1. It is also a post-hoc method.

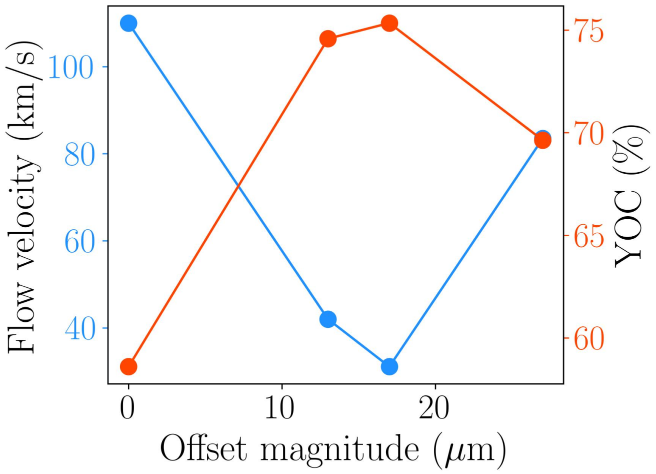

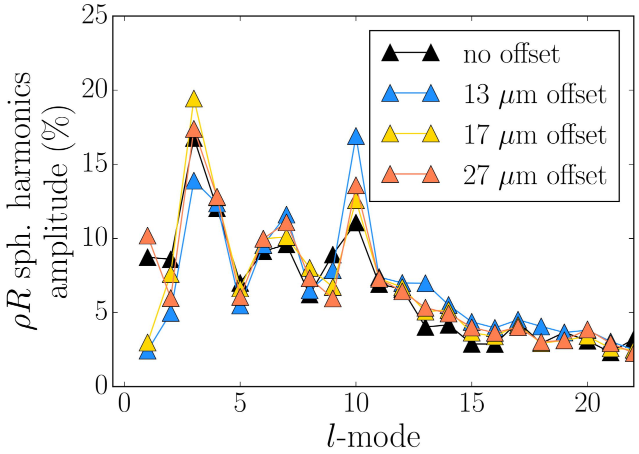

A RE-DESIGN OF THE OMEGA DPR SYSTEM IS A MORE VIABLE LONG TERM STRATEGY TO IMPROVE IMPLOSION PERFORMANCE

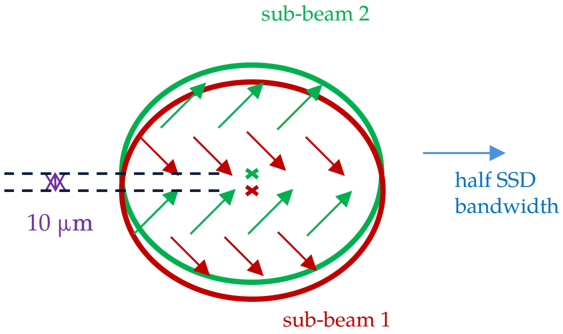

Strategy 2 :
- Re-design the DPR system on OMEGA to reduce the offset between polarizations

Pros : Allows to recover the unpolarized CBET result, effictively mitigating this source of low modes

Cons : difficult to implement, also requires to half the SSD bandwidth…

However, this anomaly does need to be corrected in the long run …

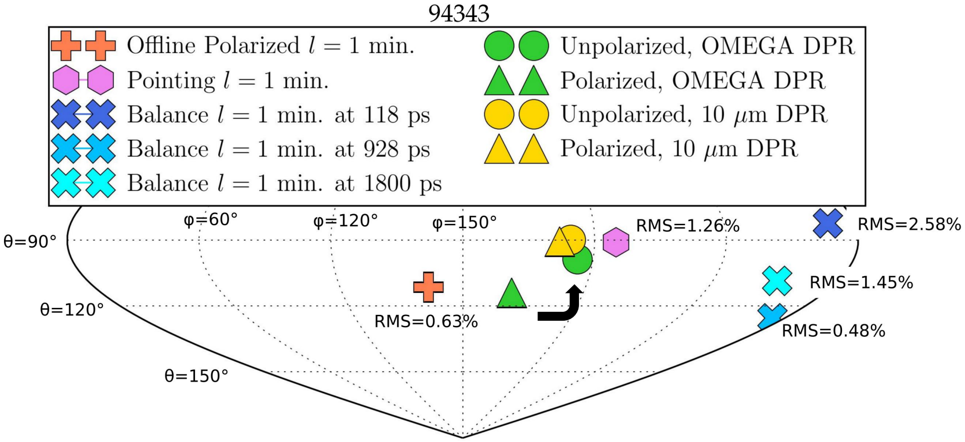

THE POLARIZED CBET MODEL HAS BEEN APPLIED TO OFFLINE ESTIMATIONS OF CBET FOR NIF

What about the polarization effect on the NIF?

Half hemisphere (96 beams) pointed at TCC, interacting in a spherical plasma with upward flow velocity at c/1000

Comparing: unpolarized quad-by-quad, unpolarized beam-by-beam, polarized beam-by-beam

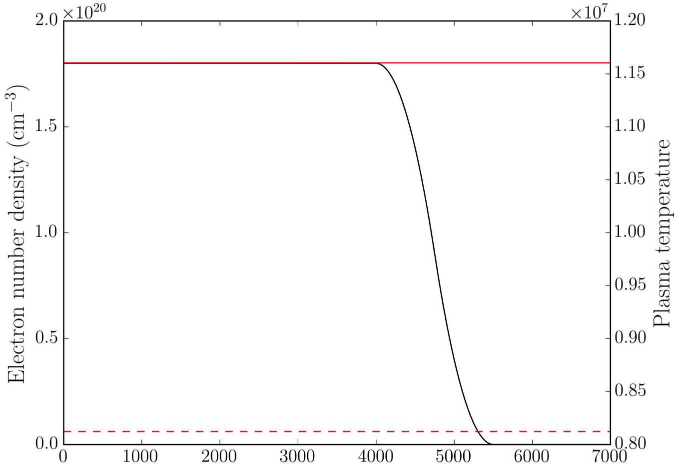

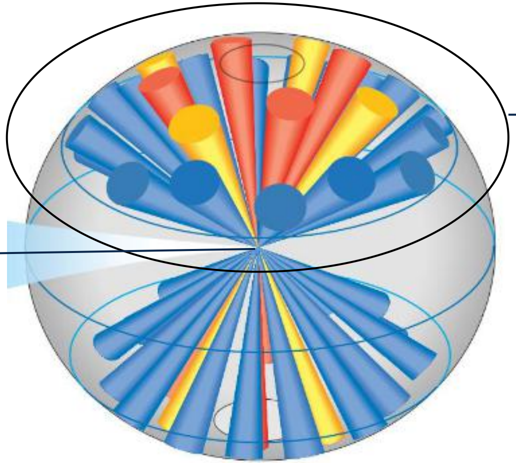

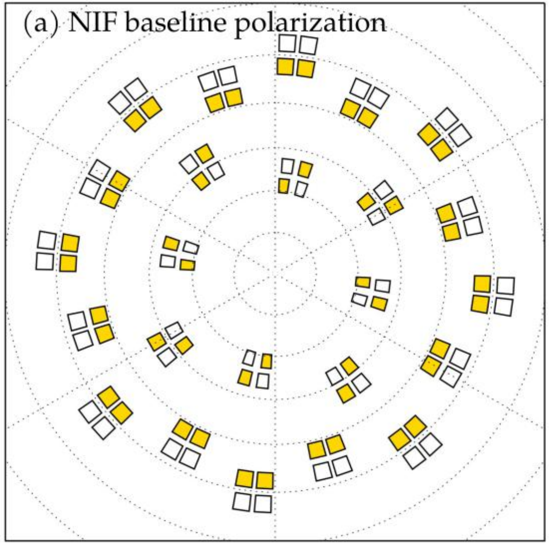

THE POLARIZATION EFFECT HAS ONLY A MODEST EFFECT ON CONE FRACTION

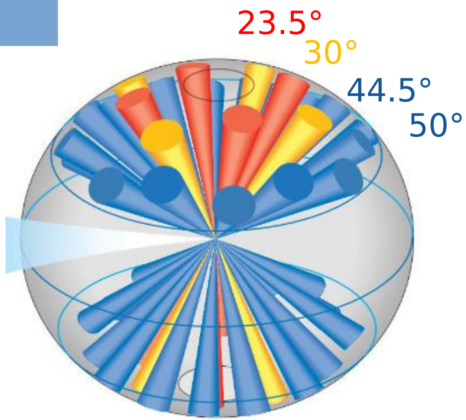

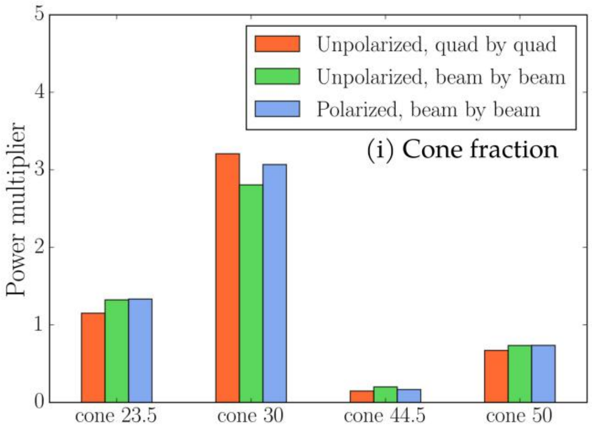

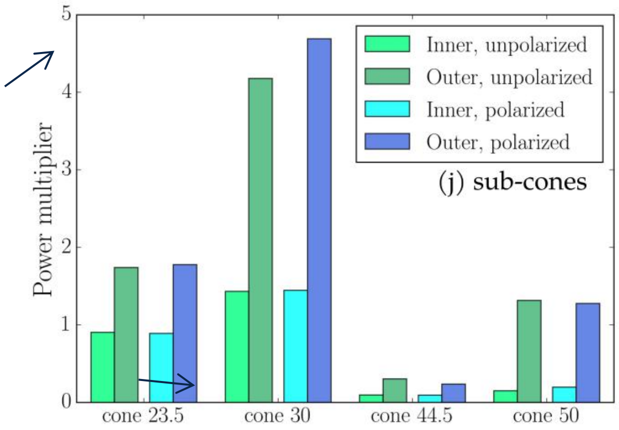

- Cone-wise, their is little effect of polarization
- In more details; polarization effect leads to more energy transfer to outer beams in cone 30 and less to outer beams in cone 44.5

THE LARGEST EFFECT ON THE DETAILS OF CBET IS THAT OF BEAM-BY-BEAM CALCULATION VS UNPOLARIZED QUADS

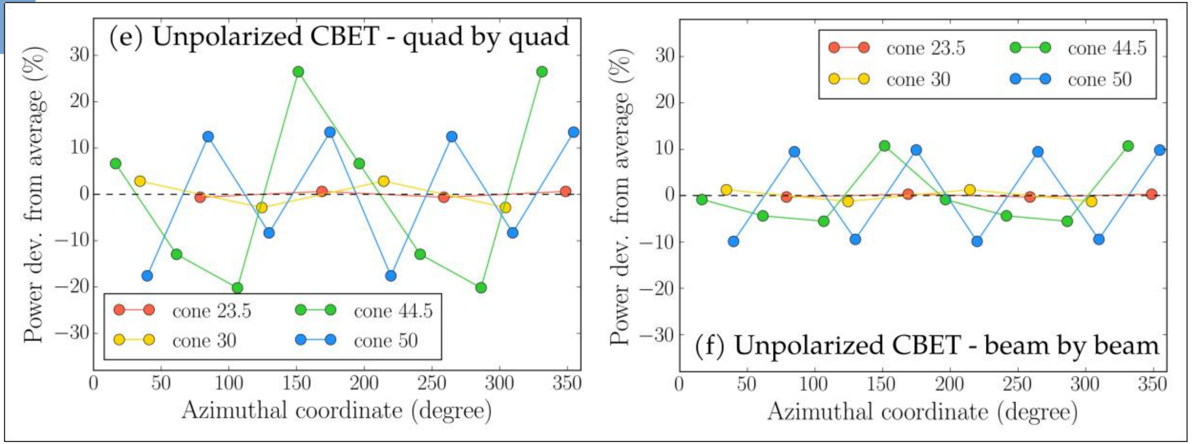

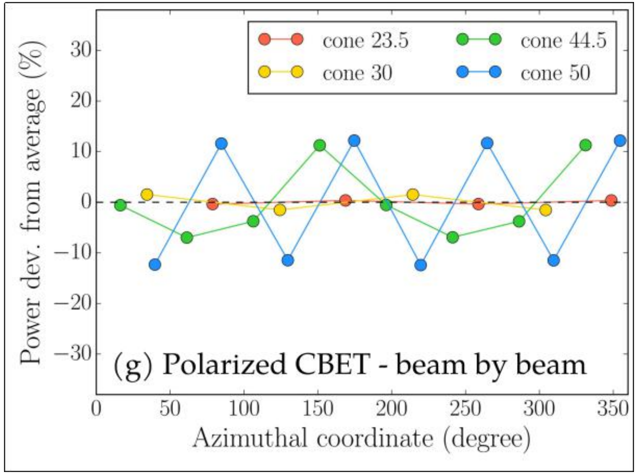

- Cone-wise, their is little effect of polarization
- In more details; polarization effect leads to more energy transfer to outer beams in cone 30 and less to outer beams in cone 44.5
- Computing the CBET beam by beam instead of quad by quad leads to less azimuthal variability in power amplification (polarized or unpolarized)

THE POLARIZATION CONFIGURATION STILL MATTERS FOR SYMMETRY

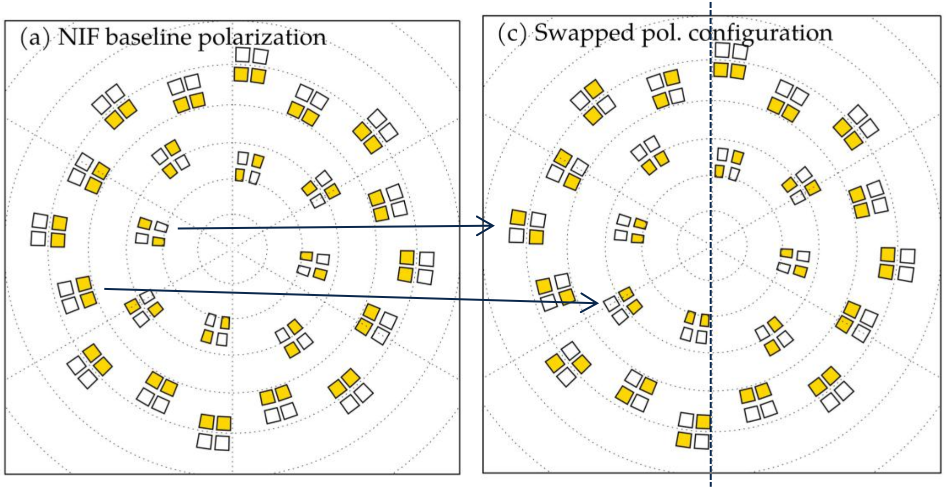

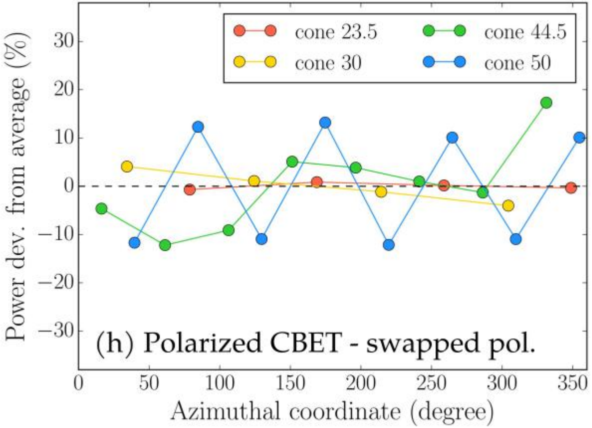

- Cone-wise, their is little effect of polarization
- In more details; polarization effect leads to more energy transfer to outer beams in cone 30 and less to outer beams in cone 44.5
- Computing the CBET beam by beam instead of quad by quad leads to less azimuthal variability in power amplification (polarized or unpolarized)
- ...but, polarization matters ! If the polarization configuration was not symmetric, the azimuthal power amplification would be non-symmetric

SIMULATION OF LASER-TARGET COUPLING EXPERIMENTS ON THE NIF SHOWS THAT THE MODELING ALSO CAPTURES DRIVE AT NIF SCALE

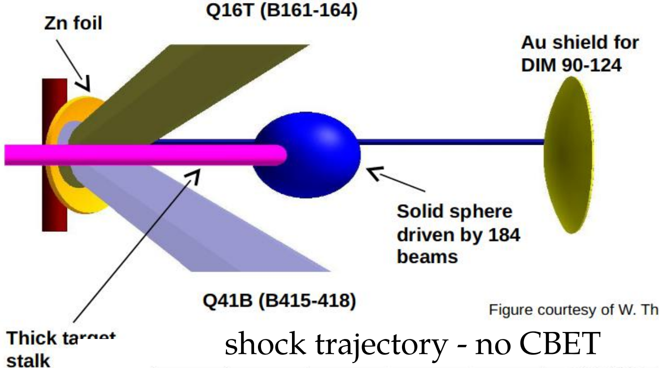

Figure courtesy of W. Theobald

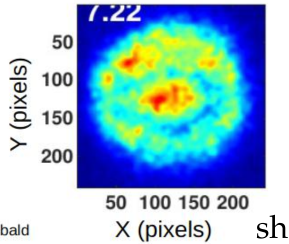

shock trajectory - no CBET

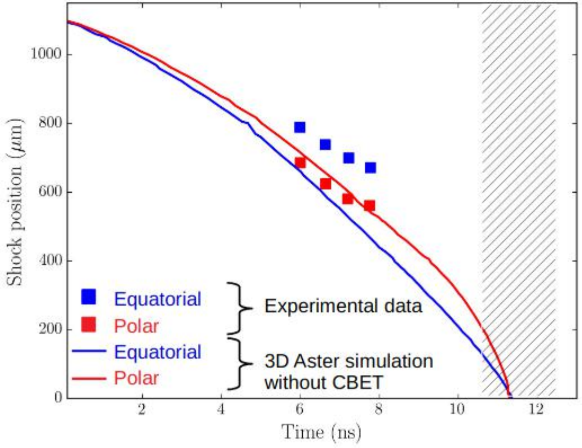

shock trajectory - CBET

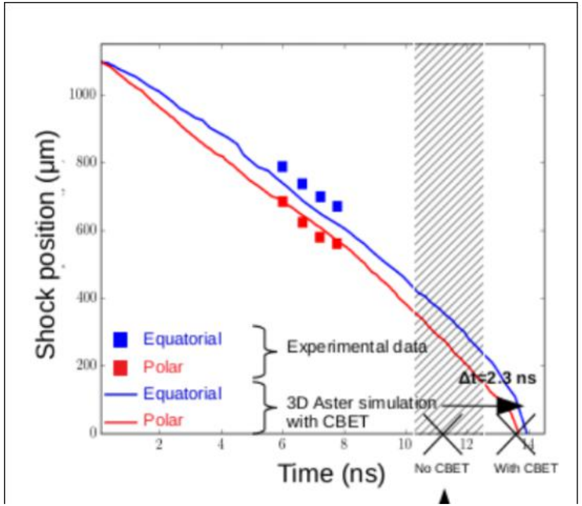

[D. Viala, poster on Monday]

The modeling also captures drive energetics correctly for NIF scale shock coupling experiments

CONCLUSIONS AND PERSPECTIVES

Conclusions:

- The CBET models implemented in ASTER/IFRIIT reproduce the large scale dynamics of implosion experiments on OMEGA, without any tuning
- ... also holds for NIF-scale direct-drive experiments => good confidence in modeling capabilities
- Some limitations remain (stalk, high mode modeling coupled to CBET)

- Polarized CBET, in addition to current low modes, explains the observed anomaly of the last 2 years of OMEGA shots
- CBET reduces yields by at least 60% on OMEGA, even worse at NIF scale => must be mitigated in a fusion driver. However, this will make current designs more vulnerable to system errors -> need more robust schemes
- Polarization effect is responsible for ~15% yield drop on OMEGA and is mostly present when other low mode sources are low
- Polarization effect is currently negligible on NIF

REASONABLE NUMERICAL EFFICIENCY IS OBTAINED BY LEVERAGING INVERSE RAY TRACING

$$u = A\exp[\imath k_0\psi]\ ,$$

$$\psi''(\tau) = \int_0^\tau \epsilon''(\mathbf{r}(\hat{\tau}))\mathrm{d}\hat{\tau}/2\ ,$$

$$A(\tau) = A(0)\left|\frac{D(0)}{D(\tau)}\right|^{1/2}\quad ,$$

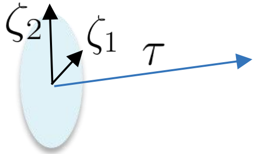

Step 1; manifold geometry
- compute the mapping from phase space (ζ_1, ζ_2) to real space (x, y)
- compute the geometric part of the laser field
- compute the Airy Integral that gives the caustic field
- compute the full Frenet frame for each sheet of each beam at each gridpoint

=> these are **geometric** factors stemming from the ray mapping
fixed during one timestep

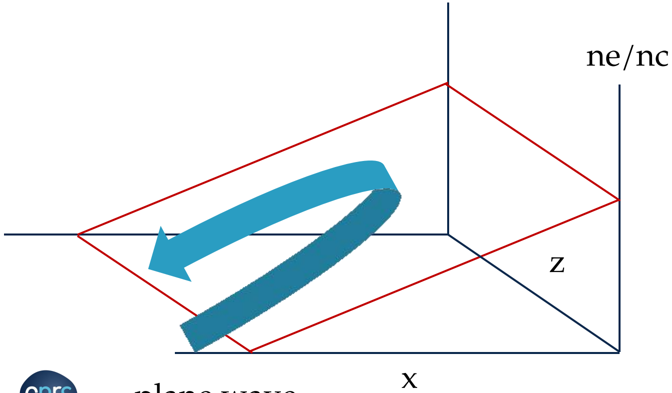

plane wave
at an angle

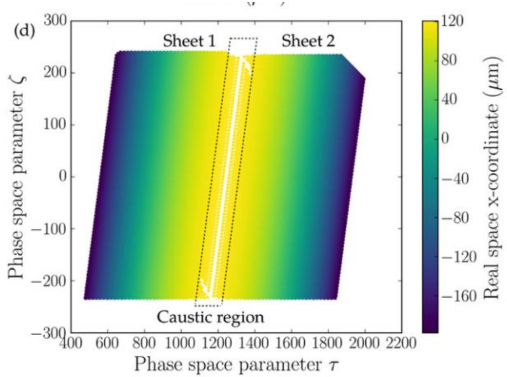

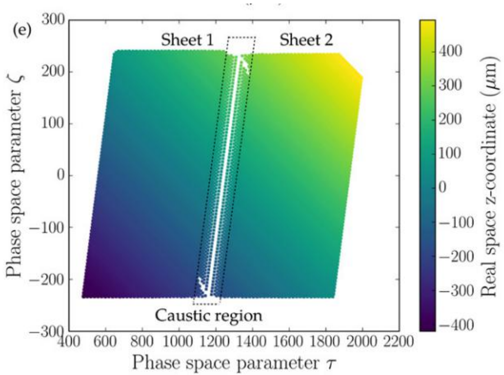

REASONABLE NUMERICAL EFFICIENCY IS OBTAINED BY LEVERAGING INVERSE RAY TRACING

$$u = A\exp[\imath k_0 \psi] \ ,$$

$$\psi''(\tau) = \int_0^\tau \epsilon''(\mathbf{r}(\hat{\tau}))\mathrm{d}\hat{\tau}/2 \ ,$$

$$A(\tau) = A(0)\left|\frac{D(0)}{D(\tau)}\right|^{1/2} \ ,$$

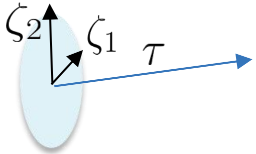

$$\begin{pmatrix}\epsilon_{i,j,\nu_n}\\ \epsilon_{i,j,b_n}\end{pmatrix} = [\epsilon'_i + \imath(\epsilon''_{0,i} f_{\mathrm{L}} + \underline{\underline{\mathcal{D}_{i,j}}})].\begin{pmatrix}1\\ 1\end{pmatrix}$$

Step 1; manifold geometry

- compute the mapping from phase space (ζ_1, ζ_2) to real space (x, y)
- compute the geometric part of the laser field
- compute the Airy Integral that gives the caustic field
- compute the full Frenet frame for each sheet of each beam at each gridpoint

=> these are **geometric** factors stemming from the ray mapping
fixed during one timestep

Step 2; fields

- compute the phase contribution to the fields
- compute the Langdon effect coefficient and the polarized CBET coupling term

Fixed point iteration with damping until convergence

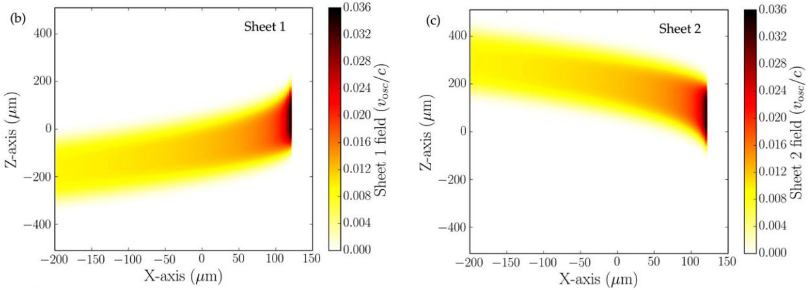

THE MODELING SYSTEMATICALLY APPROACHES THE MEASURED FLOW DIRECTION

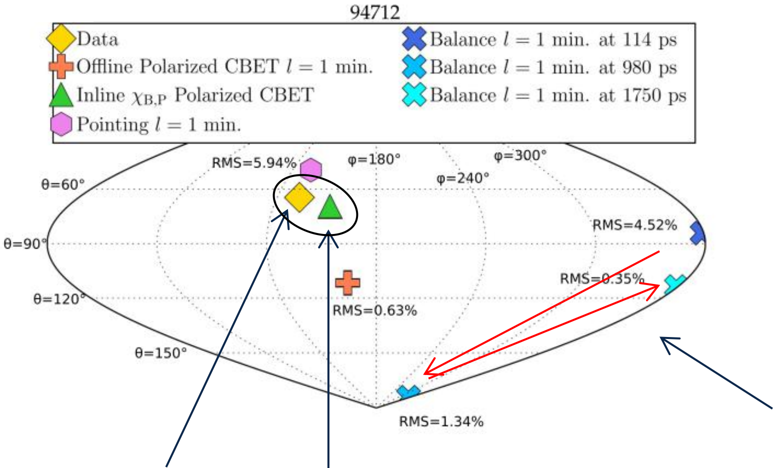

Note: the large swing in balance

Data

Simulation

94712 was dominated by pointing:
result is close to pointing anomaly

THE MODELING SYSTEMATICALLY APPROACHES THE MEASURED FLOW DIRECTION

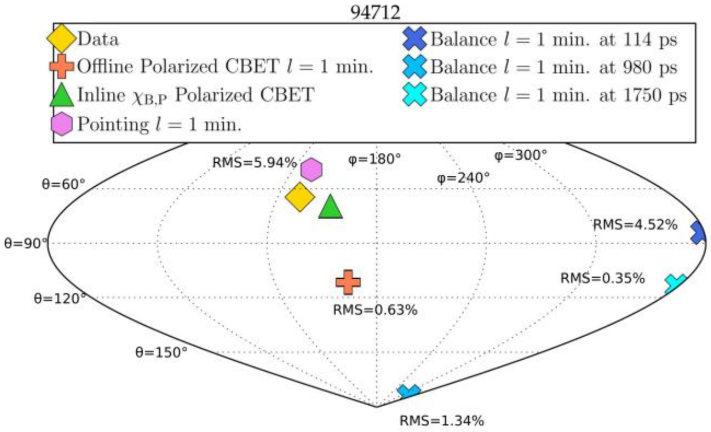

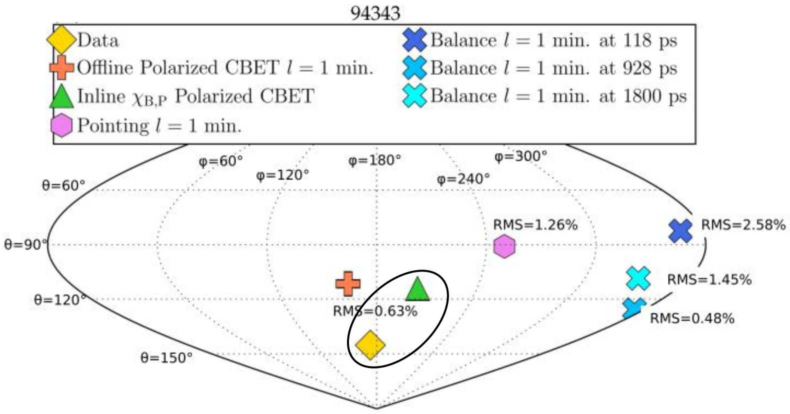

94343 had balanced low mode sources; the results is a non-trivial combination of those

Lawrence Livermore
National Laboratory